Sustainable Concretes for Transportation Infrastructure

Carolyne Namagga
Graduate Research Assistant

Rebecca Atadero
Assistant Professor

Department of Civil and Environmental Engineering
Colorado State University

July 2010

Acknowledgements

The authors gratefully acknowledge the Spray Dryer Ash that was provided for this project by the Platte River Power Authority and the funds provided for this research by the Mountain Plains Consortium, a Federal Highway Administration University Transportation Center. They also acknowledge the efforts of numerous undergraduate and graduate research assistants including Kyle Wieghaus, Doug Allen, Catherine Oakleaf, Dan Woodward, Neal Bohnen, John McWilliams, Hongyan Liu, and Thang Dao, who assisted with this project by helping to manufacture specimens and conduct testing.

Disclaimer

The contents of this report reflect the views of the authors, who are responsible for the facts and the accuracy of the information presented. This document is disseminated under the sponsorship of the Department of Transportation, University Transportation Centers Program in the interest of information exchange. The U.S. Government assumes no liability for the contents or use thereof.

North Dakota State University does not discriminate on the basis of race, color, national origin, religion, sex, disability, age, Vietnam Era Veteran's status, sexual orientation, marital status, or public assistance status. Direct inquiries to the Vice President of Equity, Diversity, and Global Outreach, 205 Old Main, (701) 231-7708.

ABSTRACT

This research focuses on the valuable utilization of spray dryer ash (SDA) and investigates its performance in concrete for structural and transportation applications. Based on the challenges associated with coal ash (including SDA) and the economic costs linked to cement production, this research seeks to develop an environmentally friendly and more cost effective concrete product by utilizing SDA in partial replacement of cement in concrete. With the exception of a relatively higher sulfur content, SDA exhibits excellent properties that are closely related to Class C fly ash and portland cement. The fineness and low carbon content properties of SDA/Class C fly ash provide potential benefits of increased strength (compressive and bond) and durability (freeze-thaw and corrosion) when used in concrete. In this study, the addition of SDA in non-air entrained concrete provides a general increase in compressive and bond strength with optimal limits ranging between 25-35% replacement. The presence of SDA produced a negligible effect on the freeze-thaw durability of the concrete, which was air entrained. Corrosion results are not as conclusive, but the 50% SDA mix provides performance similar to or slightly better than the control concrete.

TABLE OF CONTENTS

1. INTRODUCTION 1

1.1 Background 1

1.2 Research Objectives 2

1.3 Approach 3

2. LITERATURE REVIEW 5

2.1 Introduction 5

2.2 Concrete 6

2.2.1 Application of Concrete 6

2.2.2 Strength of Concrete 7

2.2.2.1 Compressive Strength 7

2.2.2.2 Bond Strength 8

2.2.3 Concrete Durability 9

2.2.3.1 Freeze-thaw 9

2.2.3.2 Corrosion 10

2.3 Cement 11

2.3.1 Cement versus Fly Ash 11

2.4 Spray Dryer Ash 12

2.4.1 Types of Fly Ash 13

2.4.2 Properties of Fly Ash 14

2.4.3 Utilization of Fly Ash 15

2.5 Fly Ash Concrete 15

2.5.1 Fly Ash and Concrete Strength 16

2.5.2 Fly Ash and Concrete Bond Strength 17

2.5.3 Fly Ash, Durability and Rebar Protection 17

3. EXPERIMENTAL SET-UP 19

3.1 Materials 19

3.1.1 Spray Dryer Ash 19

3.1.2 Other Materials 19

3.2 Mix Design 20

3.3 Compressive Strength Test 20

3.4 Bond Strength Test 21

3.5 Durability (Freeze-Thaw) Test 23

3.6 Corrosion Tests 27

4. RESULTS AND ANALYSIS 29
4.1 Compressive Strength 29
4.1.1 Early Strength Gain (0-7 days) 29
4.1.2 Rate of Strength Gain 30
4.1.3 Ultimate Strength 31
4.2 Concrete Shear Bond 32
4.2.1 Mode of Failure 33
4.2.2 Load-Slip Response 33
4.2.2.1 Specimens with 0% SDA 34
4.2.2.2 Specimens with 25% SDA 35
4.2.2.3 Specimens with 50% SDA 36
4.2.3 Bond Strength 37
4.2.5 Peak Slip and Strain 37
4.2.6 Compressive Strength of Bond Test Specimens 37
4.3 Concrete Durability (Freeze-thaw) 38
4.3.1 Weight Change 38
4.3.2 Freeze-thaw Resistance 39
4.4 Concrete Corrosion 40
4.4.1 Chloride Ion Penetration (Total Corrosion) 41
4.4.2 Rate of Corrosion Activity 42
4.4.3 Acid Soluble Chloride Content 43
5. RECOMMENDATIONS AND CONCLUSIONS 47
5.1 Conclusions 47
5.1.1 Compressive Strength 47
5.1.2 Bond Strength 47
5.1.3 Freeze-thaw (Durability) 48
5.1.4 Corrosion 48
5.2 Recommendations 48
6. REFERENCES 51
APPENDIX A: MIX DESIGN 55
APPENDIX B: COMPRESSIVE STRENGTH RESULTS 57
APPENDIX C: BOND STRENGTH RESULTS 59
APPENDIX D: FREEZE-THAW RESULTS 60
APPENDIX E: CORROSION TEST RESULTS 63

LIST OF TABLES

Table 2.1 CDOT Concrete Classification (CDOT 2008) 7
Table 2.2 Fly Ash Classification as per ASTM C618 14
Table 2.3 CCP and Fly Ash Produced/ Re-used (millions of tons) (ACAA 2010) 15
Table 3.1 Partial Chemical Composition of the Spray Dryer Ash (SDA) Used 19
Table 3.2 Concrete Material Specifications 19
Table 3.3 Summary of the PCA Absolute Volume Method for a Cubic Yard (27 ft^3) 20
Table 3.4 Non –Air Entrained Concrete Mixes (Design Strength 4500psi (31MPa)) 21
Table 3.5 Air-Entrained Concrete Mixes (Design Strength 4500psi (31MPa)) 23
Table 4.1 Summary of Bond Test Results 34
Table 4.2 Average Results of Peak Loads (kips), Peak Slips (in), and Rebar Strains 37
Table 4.3 28-day Mean Compressive Strengths (psi) for the Bond Test Specimen 38
Table 4.4 Weight (lb) and Weight Change (%) Specimens Over N Cycles 39
Table 4.5 Durability Factors and Relative Durability Factors 40
Table 4.6 Average Corrosion Potentials (Against Reference Electrode) of Specimens 41
Table 4.7 Probability of Corrosion (ASTM C876) 42
Table 4.8 Results of Acid-Soluble Chloride Testing 44

LIST OF FIGURES

Figure 2.1 Overall CCP 2007 Production (ACAA 2007) 5
Figure 3.1 Compression Testing Machine 21
Figure 3.2 Beam/ Rebar Specimen Set-up 22
Figure 3.3 Schematic of Beam- End Specimen and Apparatus 22
Figure 3.4 Air Entrainment Testing Apparatus (Volumetair) 23
Figure 3.5 Concrete Prisms for Freeze-thaw Testing 24
Figure 3.6 Schematic of Apparatus for Transverse Frequency Test 25
Figure 3.7 Picture of Apparatus for Frequency Testing 25
Figure 3.8 LabView Program 26
Figure 3.9 Timber Forms and Rebar for Corrosion Specimens 27
Figure 3.10 a) Corrosion Specimens b) with Plastic Dams and Epoxy 27
Figure 4.1 Concrete Test Specimens at Failure 29
Figure 4.2 Early Compressive Strength of SDA Concrete 30
Figure 4.3 Compressive Strength Against Age of Concrete 31
Figure 4.4 Compressive Strength Against SDA Concrete (for 28 and 56 days) 32
Figure 4.5 Beam Loaded Indicating Shear Bond failure 33
Figure 4.6 a) Load vs. Slip for Beam (B1) b) Load vs. Slip for Beam (B2) 35
Figure 4.6 c) Load vs. Slip for Beam (B3) 35
Figure 4.7 Load vs. Slip for Beams (B4, B5, B6) with 25% SDA 36
Figure 4.8 Load vs. Slip for Beams (B7, B8, B9) with 50% SDA 36
Figure 4.9 Change in RDM (%) of SDA Concrete vs. Number of Cycles 40
Figure 4.10 Total Corrosion vs. Concrete Age 42
Figure 4.11 Macrocell Current vs. Time of Testing (Corrosion Rate) 43
Figure 4.12 Chloride Content (% Mass of Concrete) vs. Depth 44

LIST OF ABBREVIATIONS

ACI	American Concrete Institute
ASTM	American Standards of Testing Materials
CCP	Coal Combustion Products
C-S-H	Calcium Silicate Hydrate
CSU	Colorado State University
DF	Durability Factor
EPA	Environmental Protection Agency
EPRI	Electric Power Research Institute
FGD	Flue Gas Desulfurization
LOI	Loss On Ignition
PCA	Portland Cement Association
RDF	Relative Durability Factor
RDM	Relative Dynamic Modulus of Elasticity
SDA	Spray Dryer Ash
USGS	United States Geological Survey

EXECUTIVE SUMMARY

This research focuses on the valuable utilization of spray dryer ash (SDA) and investigates its performance in concrete for structural and transportation applications. Based on the challenges associated with coal ash disposal and the economic and environmental costs linked to cement production, this research seeks to provide an environmentally friendly and more cost effective concrete product by utilizing SDA in partial replacement of cement in concrete.

Residual products of energy production through coal burning such as fly ash and SDA exhibit excellent properties that are closely related to portland cement and are vital to the concrete industry. SDA is similar to fly ash in many ways and most closely resembles Class C fly ash. It is a relatively new product, and limited research has been done on its application. This study is based on the hypothesis that it will perform similarly to Class C ashes.

The fineness and carbon content of this type of fly ash/ SDA are key properties in determining its reactivity and strength characteristics. The fineness of the SDA reduces the porosity of the concrete and increases the volume-to-surface area ratio needed for the pozzolanic reaction, though it affects the amount of air entrained in the concrete. The low carbon content of SDA, however, provides for an increase in the workability and effectiveness of the air entrainer in the concrete, hence improving its reactivity and strength development. With the exception of the relatively high sulfur content, the quality of the SDA produced is quite safe for engineering use since it is very low in hazardous minerals (EPRI 1998).
This report describes research to study the use of large volumes of spray dryer ash in concrete. During the project spray dryer ash obtained from a local power plant was used in the concrete tests. Varying amounts of SDA were used in given mixes of concrete as a partial replacement of the cement (binder) and fine aggregate (filler). Several design mixes were prepared, cured, and tested for their compressive and bond strengths, durability (freeze-thaw), and corrosion properties. Test results were analyzed and compared with the control concrete in order to draw conclusions about how the SDA can be best used.

Presented in this report are the results for the strength (compressive and bond) tests and durability (freeze-thaw and corrosion) tests. The compressive strength tests show a general increase in the ultimate strength of concrete with the addition of SDA with the best strength results obtained at 25-35% SDA replacement. Beyond 35% SDA replacement reduced strengths are observed, although they still achieve the required design strength. The best results in the bond strength are obtained when SDA utilized in concrete is limited to 25% replacement. Doubling this quantity of SDA (50%) results in reduced bond strength; however, it still exceeded the strength of the control specimens. The freeze-thaw test results indicate that replacing proportions of cement with SDA requires more air entraining admixture. Despite the need for more air entrainment, utilization of SDA produces a negligible effect on the freeze-thaw durability of the concrete. Corrosion results are less conclusive. The 25% SDA mix appears to be worse than the control mix, while the 50% SDA mix is slightly better. In general, the addition of SDA provides modest benefits when used in certain proportions and demonstrates great potential for utilization as a structural material in transportation infrastructures.

1. INTRODUCTION

1.1 Background

This research focuses on the potential for the valuable utilization of spray dryer ash (SDA) as a binding agent in concrete and investigates its performance in concrete for structural and transportation applications. SDA is a byproduct of electricity generation from coal and the scrubbing process used to remove sulfur from power plant emissions. Based on the challenges associated with disposal of all types of coal ash, including SDA and the economic and environmental costs linked to cement production, this research seeks to provide an environmentally friendly and more cost effective concrete product by utilizing SDA as a partial replacement of cement in concrete. Cement production is a rather expensive venture, yet there is an abundance of coal ash such as SDA and fly ash that is disposed off in landfills that could be utilized positively.

Spray dryer ash, also known as spray dryer absorber material, is a by-product of coal energy production, obtained from the flue gas desulfurization (FGD) process. The SDA considered in this study is a self-cementing coal ash material obtained in Northern Colorado at the Rawhide Power Station, managed by the Platte River Power Authority. This material is unique to the mid-western and western regions of the United States due to the unique FGD process, commonly referred to as 'Scrubbing,' used in the removal of sulfur dioxide from the residual gases during the coal based energy production processes. The SDA material is a highly alkaline residual fly ash that is contaminated with sulfur in this scrubbing process (Hoffman *n.d.*), disqualifying it from the Class C specification for fly ash use in concrete (ASTM C618) that requires the sulfur content to be less than 6%. With the exception of the high sulfur, the quality of the SDA produced is quite safe for engineering use since it is very low in hazardous minerals (EPRI 1998). Despite the undesirably high sulfur content, this research will investigate its potential for beneficial use in concrete.

Concrete, which is one of the most widely used construction materials, is a composite of aggregate, cement and water. Concrete is produced at an estimated global rate of five billion cubic yards per year. It is the second most widely consumed substance on earth, after water (PCA 2006). It has been used as one of the major construction materials in some of the world's largest infrastructure such as the Hoover Dam[1], Petronas Towers[2], Jin Mao Tower[3] and Dames Point Bridge,[4] and it is a major component in much of the highway infrastructure. For example, 67% of the U.S. Interstate highway and bridge system has been built of concrete (NBI 1994).

Concrete, together with reinforcement, is well known for its high strength development, resistance to large magnitudes of loads, and small deformations when compared to asphalt. When used in pavement construction, concrete provides an average useful life of about 20-30 years before needing rehabilitation; compared to an asphalt pavement that has a service life of 8-12 years (PCA 2009a). Construction of a concrete pavement requires a higher initial investment, but it has a very low maintenance cost as compared to asphalt (PCA 2009a). A high initial investment could be reduced by utilizing recycled materials and waste products in substitution or replacement of cement. An extended service life and reduced life cycle cost could also be actualized when these materials are used for bridge construction (Daigle *et al.* 2006).

---

[1] 1244ft long, 726.4ft high (2nd highest in the U.S.) dam located on Colorado river at Arizona-Nevada border
[2] 1378 ft high skyscraper building in Kuala Lumpur, Malaysia
[3] 1371ft high skyscraper building, Shanghai, China
[4] 2 miles long bridge, spans St. John River, Jacksonville, Florida

Portland cement production poses challenges of excessive energy usage and depletion of natural resources. Cement is chemically manufactured from calcium, silicates, and aluminates in a process that releases carbon dioxide as a by-product into the atmosphere and depletes the earth of mineral resources (Bye 1999). In 2007, the world production of cement was approximately 2.6 billion metric tons, with 127 million produced and consumed within the United States (USGS 2008). But when a ton of coal ash is used in place of cement, 55 gallons of oil required to produce a single ton of cement is saved, and an equal amount of carbon dioxide that would be produced by the manufacturing process is prevented from entering the Earth's atmosphere (ACAA 2009), hence making a significant positive impact on the environment and preservation of natural resources.

Portland cement is a hydraulic material, and it exhibits properties similar to the residual waste (fly ash and SDA) obtained from coal energy production. Fly ash has produced excellent results when used in concrete, and in many instances concrete mixes including fly ash have outperformed standard concrete. There exist different types of fly ash, and a lot of research has been conducted to investigate its beneficial application in several engineering industries. SDA is closely related to Class C fly ash. It is a relatively new product that and has not yet been the subject of extensive study. However, based on the previous success of Class C fly ash in concrete, it appears that SDA could provide a suitable substitute for portland cement and an environmentally friendly solution to the concrete industry.

Fly ash has, for so many years, been a hazard to the environment. Several millions of tons of fly ash and SDA are disposed off annually in landfills and ponds, raising concerns of ground water contamination and health hazards to the environment (EPRI 1998). Despite the disposal challenge, these materials possess very excellent properties that produce distinct benefits when added to traditional concrete mixes such as improved workability, reduced permeability, increased ultimate strength, and reduced heat of hydration (King 2005).

In an attempt to improve the environment and enhance the concrete industry, it is essential to provide more sustainable and 'green' options as solutions and better alternatives to existing products. Extensive research has been done in an attempt to make concrete products more sustainable and cost effective. This research has included recycling and utilizing valuable waste products such as car tires, glass, waste plastics, slag, and fly ash, which have been used in kilns to improve the cement manufacture process and in concrete production. The utilization of SDA is another attempt at reducing concrete's carbon footprint on the environment, thereby enhancing the sustainability of the transportation infrastructure constructed with concrete.

1.2 Research Objectives

The main objective for this work was to carry out preliminary research on four different properties that are instrumental to the transportation industry to demonstrate the viability of SDA as a suitable partial alternative for cement in concretes. A more in-depth study into these properties would be recommended. The research described in this report will only demonstrate the suitability of SDA for use in transportation concretes by the following:

- Investigating and recommending quantities that would provide suitable results in terms of compressive strength when SDA is used as a substitute for cement.
- Quantifying the bond strength behavior of SDA concrete through laboratory testing.
- Studying the durability of SDA concrete with an emphasis on the freeze-thaw performance of the concrete.
- Examining the corrosive behavior of rebar embedded in SDA concrete when exposed to a chloride environment.

1.3 Approach

To meet the above objectives, a research team assembled to carry out experimental work on the SDA concrete. This work was carried out in the Concrete Laboratory and Engineering Research Center at CSU through laboratory testing of specimens in accordance with the relevant ASTM standards. Concrete samples with variable quantities of SDA were prepared, cured, and tested for their strength, durability, and corrosion properties. The results from these investigations are analyzed and detailed within this report.

This report provides an overview of previous studies done on SDA and fly ash in concrete (section two), an outline of the experimental set-up of the research work (section three), an analysis of the results (section four) and conclusions and recommendations for further studies (section five). Design tables and raw data from testing are appended at the end of the report.

2. LITERATURE REVIEW

2.1 Introduction

Spray dryer ash (SDA) is one of the many residual products of coal-based energy production. Collectively, these products have been termed as coal combustion products (CCP). The other CCPs include fly ash, FDG gypsum, boiler slag, and bottom ash.

Numerous research projects have been conducted on the engineering application of these products, particularly with fly ash. Engineers have utilized fly ash as an alternative product in replacement or (partial) substitution of cement in concrete, as a structural fill, and as road base aggregates. CCPs have also found application in many other sectors, such as agriculture, mining, cement production as raw feed for the clinker, and waste stabilization, as illustrated in Figure 2.1.

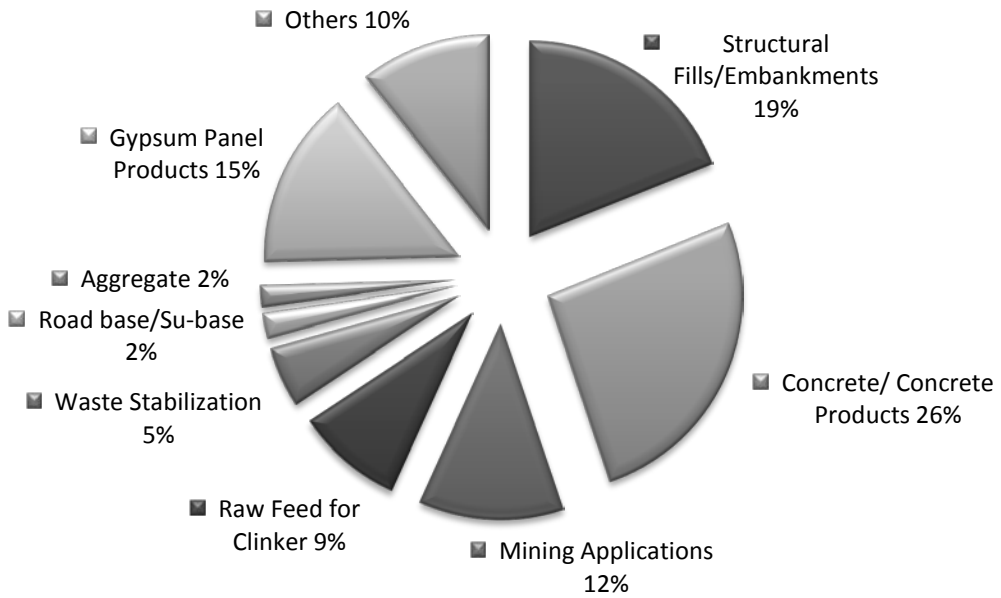

Figure 2.1 Overall CCP 2007 Production (ACAA, 2007)

SDA material is a relatively new CCP that has been in existence since the 1980s when power plants built after 1978 employed the use of the flue gas desulfurization (FGD) process to limit the release of sulfur dioxide in compliance with the Clean Air Act (EPRI 2007). Therefore, in comparison to fly ash, there is not much research on the beneficial use of SDA. For this reason, this literature review will include previous work with SDA when available, but will also draw from previous work with fly ash in concrete.

Fly ash is very useful in the concrete industry due to its pozzolanic behavior in forming cementitious bonds. Concrete is characteristically defined by the strength of these cementitious bonds created between the aggregates. The strength of these bonds is determined by the nature and type of pozzolanic material used within the concrete.

A pozzolan is an alumino-siliceous material, which in the presence of water reacts with calcium hydroxide to form compounds possessing cementitious properties. Generally, they have the ability to set at room temperature without the use of any retarders or accelerators/ superplasticizers (King 2005). Several types of pozzolans exist, in addition to fly ash, such as silica fumes, calcined clay (metakaolin), ground granulated blast furnace slag (slag), and of recent production SDA. The pozzolans can be acquired

naturally when mined directly as volcanic tuffs, manufactured as metakoalin, retrieved as an industrial by-product, or acquired from burning rice hull (Malhotra 1986). This research focuses only on SDA and its use in concrete.

2.2 Concrete

Concrete is a composite material comprising aggregates and any binder/pozzolan mixed together in the presence of water to form a hardened structure of durable quality and strength. The most commonly used binder is portland cement. Other binders that contain pozzolans such as fly ash (and SDA), silica fumes, ground granulated blast furnace slag, and metakoalin can be used in complete substitution or partial replacement of portland cement (Malhotra 1986).

Some admixtures such as super-plasticizers or retarders can be added to any concrete to facilitate or retard the hydration reaction process of the concrete. When these admixtures are added to the concrete, they modify the concrete and form different types that are specific to the user's application. Such modified concrete could be referred to as high strength, high performance, shotcrete (Garshol *et al.* 2007), and many other names, such as asphalt concrete, lime concrete, and glass concrete (Poutos *et al.* 2008) when the cement or aggregates are substituted for other materials of similar properties.

2.2.1 Application of Concrete

Concrete is widely used in the construction and highway industries. An estimated global rate of five billion cubic yards per year of concrete is produced (ACAA 2009). In the United States, concrete has found a great application in bridge and pavement infrastructure. Presently, more than 50% of the bridges in the United States are constructed out of prestressed concrete (TRB 2009).

Concrete has been used in isolation, referred to as mass concrete, or together with steel materials to form reinforced or pre-stressed concrete. It has also been used in masonry to manufacture concrete blocks or pavers and other concrete products such as pipes, culverts, and highway barriers (PCA 2009b). Concrete has been used in the design and construction of structural elements such as columns, beams, slabs, piles/caissons, shear, and retaining walls in buildings and piers, towers, and pavements in highway construction. It has been used in the construction of other structures such as dams, swimming pools, water tanks and silos. Concrete gains its popularity, in many instances, from its high strength development and its high resistance to impact and bending.

'Modified' concrete has been used widely in bridge/highway construction and in other applications that require early strength development and fast setting of concrete. For example, glass concrete has been shown to improve the thermal insulation of buildings (Poutos *et al.* 2008). Limecrete (lime used with concrete) has been used in flooring systems to enhance under-floor insulation and eliminate floor dampness in the interiors of buildings. Limecrete is used in areas that are not exposed to weather conditions. Shotcrete (concrete sprayed at high pressures) is normally used in tunneling, in areas where seepage is a concern, areas with high water tables, and against vertical soil or rock surfaces (Garshol *et al.* 2007). In a bid to conserve the environment, sustainable materials such as fly ash have been utilized in modifying the concrete. Concrete itself has been recycled and utilized as aggregate in new concrete or in a road sub-base layer (Buck 1977).

2.2.2 Strength of Concrete

2.2.2.1 Compressive Strength

Concrete members are designed based on the concrete's compressive strength. When improperly designed, concrete members will ultimately fail due to the occurrence of significant tensile loads. The presence of smaller tensile loads in concrete will induce cracks, which may cause serviceability limit states to be reached.

Several classes of concrete strength are utilized based on their intended applications. For example, the strengths will vary depending on whether concrete is for non-structural (general) use or for structural applications such as drilled piers, concrete pavements (decks), girders, or repairs. Concrete may also be specified to achieve high strength or early strength requirements. The typical range of strength used for conventional reinforced concrete is 3000-4000 psi (21-28 MPa) while that used for prestressed (high strength) concrete is 5000-6000 psi (35-41 MPa). Higher concrete strengths provide for a reduction in weight of the members, and they experience smaller volume changes. Volume changes can affect the proper functioning of the members, for example causing a loss of prestress in prestressed concrete members (Tonias 2007).

Strengths required for transportation use tend to range between 4000-6000 psi (28-41 MPa). The AASHTO LRFD specifications (1994) provide minimum requirements for the classes of strength to be used for different applications. The Colorado Department of Transportation (CDOT) has narrowed down the AASHTO specifications to suit Colorado environmental conditions. CDOT has the concrete classes shown in Table 2.1. The classes specify the required field compressive strength at a given age of the concrete.

Table 2.1 CDOT Concrete Classification (CDOT 2008)

Concrete Class	Required Field Compressive Strength (psi)	Cementitious Content: Minimum or Range (lbs/yd^3)	Air Content Range (%)	Water Cementitious Ratio: max / range
B	4500 at 28 days	N/A	5 - 8	0.45
BZ	4000 at 28 days	610	N/A	0.45
D	4500 at 28 days	615 – 660	5 - 8	0.44
DT	4500 at 28 days	700	5 - 8	0.44
E	4200 at 28 days	660	4 - 8	0.44
H	4500 at 56 days	580 – 640	5 - 8	0.38 – 0.42
HT	4500 at 56 days	580 – 640	5 - 8	0.38 – 0.42
P	4200 at 28 days	660	4 - 8	0.44
S35	5000 at 28 days	615 – 720	5 - 8	0.42
S40	5800 at 28 days	615 - 760	5 - 8	0.40
S50	7250 at 28 days	615 - 800	5 - 8	0.38

Each of the classes (Table 2.1) is designated for a specific purpose. For example, Class B is an air entrained concrete and is utilized for general use while Class DT is used for deck resurfacing and repairs. The final three classes in the table, classes S35-S50 are specified for high strength use in structural applications such as bridge girder and pier construction (CDOT 2008). It is important that the concrete utilized has a composition that limits the effects of forces such as shear, bending, torsion, and deformation phenomena such as concrete creep, fatigue, shrinkage, or thermal expansion, and yet maintains sufficient

strength for the duration for which the structure was designed. This duration is usually 10-20 years for concrete pavements (Tonias 2007).

2.2.2.2 Bond Strength

For reinforced concrete to function as a structural material, it is important to maintain composite action, which requires the transfer of load between the concrete and steel. This ability to transfer load is referred to as the bond. The load transfer between concrete and rebar occurs through friction (local bond-slip relationship) and the mechanical interaction between the reinforcing bar and the surrounding concrete. Mechanical interaction is the dominant mechanism of load transfer at small to moderate slip levels, but friction dominates at extreme slip levels and immediately upon load reversal. For reinforced concrete structures subjected to moderate loading, the bond stress capacity (mechanical interaction) of the system exceeds the demand, hence very small movements are observed between the reinforcing steel and surrounding concrete. However, for systems subjected to severe loading, localized bond demand may exceed the bond capacity and result in localized damage and significant movement between the steel and concrete (Lowes *et al.* 2004).

Experimental investigation indicates that the bond response is determined by a number of parameters and system variables. These parameters include composite material state, steel and concrete material properties (compressive strength, tensile strength, and steel yield strength), steel ratios, and thickness of concrete cover. The bond strength response is characterized as a function of compressive strength and bar size. It is determined by slip damage of concrete at the rebar-concrete interface. Loss of bond strength typically results from the development of localized cracks or due to concrete-rebar shear. Bond failure is due to tensile cracking or shearing of concrete (Lowes *et al.* 2004). The relationship between the bond strength (τ) and compressive strength (f_c) can be defined (Eligehausen *et al.* 1983) by

$$\tau \propto k(f_c)^{\beta} \qquad \text{for } ({}^{1}/_{3} \leq \beta < {}^{1}/_{2}) \tag{2.1}$$

The standard (ACI 2008) simplifies the bond strength relationship above by equating $\beta = 1/2$ and a constant, k, that is dependent on the serviceability requirements for the different flexural members. Under initial loading, the bond stresses are largest near the surface and tend to zero at the embedded end. As the loaded reinforced concrete approaches its bond failure, the stresses along the reinforcing bar become uniformly distributed. This maximum bond strength (τ_{max}) given below (2.3) is computed from the equilibrium relationship (2.2) between maximum (bond/ tensile) load applied to the bar and the internal bond slip load

$$A_s f_y = \pi d_s l_s \tau_{\max} \tag{2.2}$$

and is defined as a function of bar diameter (d_s), development (slip) length (l_s) and the steel's yield strength (f_y) (Nawy 2000):

$$\tau_{\max} = \frac{A_s f_y}{\pi d_s l_s} = \frac{f_y d_s}{4 l_s} \tag{2.3}$$

Experimental investigations have considered the response of bars ranging in size from No. 6 to No. 10. Variables such as the cyclic load history, type of concrete confinement, level of concrete damage, and strain history will also determine the maximum strength attained (Lowes *et al.* 2004).

Consequently, it is important to have sufficient anchorage and flexural bond length that will provide good development of local bond slippage, a well-defined bond zone length, and minimize cracking in the concrete. As a result, the reinforcement should be able to attain its yield strength without failure of the bond (Nawy 2000).

2.2.3 Concrete Durability

There are numerous durability concerns faced by concrete, and these include alkali-aggregate reaction; chemical attack by sulfates, chlorides and other aggressive chemicals; freezing and thawing; and severe exposure conditions (Joshi and Lohtia 1997). Concrete should be designed to resist weathering action, abrasion, and chemical attacks, while maintaining its engineering purpose. When these concerns are not addressed properly, they can cause serviceability problems, concrete deterioration, and corrosion of the rebar imbedded within the concrete (Joshi and Lohtia 1997). This report focuses on the freeze-thaw challenge and rebar corrosion problem in reinforced concrete.

2.2.3.1 Freeze-thaw

Concrete is most vulnerable to frost during its early ages (first week) due to relatively high capillary water content and its low strength. It is essential to protect the premature concrete from the initial freezing cycles. When exposed to very low temperatures, long periods of freezing, and/or subjected to frequent cycles of freeze-thaw, concrete is at great risk of durability failure if no measures are taken. Damage arises from the freezing of the pore water within the concrete that is accompanied by its expansion. In mitigating this effect, air entrainment admixtures are utilized to provide extra air voids that provide space for the freezing water to expand into, without causing damage to the concrete (Richardson 2002).

The amount of air content required depends on the volume of frozen water to be accommodated, which is a function of the permeability and porosity properties of the concrete. It is minimized by lowering the water-cementitious materials ratio used for the concrete (Richardson 2002). The amount of air required to provide adequate freeze-thaw resistance is also dependent on the nominal maximum size of aggregate and the level of exposure. The required air content will decrease with an increase in the maximum aggregate size due to a reduction in the mortar content. Concrete mixes with a maximum aggregate size of 3/4 in (20 mm) containing air entrainment are designed to produce an air content approximately equal to 4-6% of the concrete volume (ACI 211 1991).

Concrete subjected to alternate cycles of freezing and thawing experience primarily two types of deterioration, namely surface scaling and internal cracking. Scaling is the most frequently observed form of deterioration, and it is the progressive loss of small particles of mortar on a concrete surface subjected to alternate freeze-thaw cycles, hence exposing the coarse aggregates. Cracking is formed due to the internal pressures generated by the action of frost within the hardened concrete. The resistance of the concrete to frost is dependent on various factors affecting the aggregate-paste interface such as the strength of the interface, degree of saturation, creep and the pore structure of the paste (Pigeon *et al.* 1995).

Internal cracking is uncommon nowadays since most of this concrete has been protected by the use of air entrainment, but is typical in the laboratory for concrete specimens that are fully saturated. The test method described in ASTM C666 ascribes to measurement of the fundamental frequency (and relative dynamic modulus of elasticity), whose reduction is an indicator of the extent of internal cracking in concrete specimens (Pigeon *et al.* 1995).

This reduction in the measurement can also be influenced by the surface scaling when the concrete specimens are subjected to freezing in the soaked water. The transverse fundamental frequency is a

function of the mass of the specimen; heavier specimens will have a higher frequency. Subsequently the scaling effect, when severe, could significantly reduce the mass of the specimen, hence reducing the durability factor below 60% without showing any significant micro-cracking (Pigeon *et al.* 1995).

The fundamental frequency reflects the internal disruptions within the concrete due to deficiencies in the air-void characteristics or nature of aggregates while a weight loss is due to the scaling effect. A reduction in fundamental frequency can occur without a decrease in the weight loss and vice visa. ASTM C260, C494, and C1017 require that the relative (in relation to reference/control concrete) durability factor of air entrained concrete with admixture under investigation should be at least 80%, but no minimum durability factor or other requirements are given in the ASTM standards. Wang (2009) in his research defines a good durable low permeability concrete as one that attains a durability factor of at least 85%.

The introduction of air entrainment in concrete involves a certain sacrifice in concrete strength though it enhances its durability. Checks and controls on selected materials are essential to ensuring that the desired strength for the desired design life in the given exposure conditions is attained. Design guides have also made adjustments to the mix proportions to ensure a feasible compromise on the strength and durability of concrete (Kosmatka *et al.* 2002).

2.2.3.2 Corrosion

The corrosion of steel rebar is the primary and most costly form of deterioration experienced by reinforced concrete bridge structures. In the United States, maintenance and rehabilitation costs for deficient bridges are very high and are measured in billions of dollars. (Wipf 2006).

The risk of corrosion of steel rebar can be minimized if a sufficient depth of concrete cover is provided for the steel. It can also be minimized if the concrete is well designed, since concrete is highly alkaline (pH ~12) and can provide a protective layer for the embedded steel. However, when the concrete is subjected to corrosive conditions, oxygen, chemicals such as chlorides, sulfates, carbonates, and moisture can ingress through the pores to reach the rebar surface and alter the alkalinity of the concrete and cause the breakdown of the passive layer, hence causing corrosion of the steel (Bavarian *et al.* 2006).

Ingress of chlorides such as sodium chloride (de-icing salts) is one of the major causes of steel rebar corrosion in concrete utilized in the transportation industry. The corrosion deterioration would begin with the penetration of chloride ions into the concrete, then the breakdown of the passive layer, more acute corrosion of the rebar, micro cracking, and eventually spalling of the concrete (Bavarian *et al.* 2006). The breakdown of the passive layer can be brought about by many other interactions such as structural, physical, chemical, and environmental considerations. For example, a structural failure of the reinforced concrete can create cracks within the concrete that would eventually expose the embedded rebar to corrosion. When the rebar is exposed to the environment, the steel is subjected to oxidation and ferrous ions (rust) are formed, as shown in equation (2.4):

$$2\mathrm{Fe}^{2+} + 3H_2O = \mathrm{Fe}_2\mathrm{O}_3 + 6\mathrm{H}^+ \tag{2.4}$$

The penetration of the chloride ion among other properties such as the resistance to sulfate attack and alkali-silica reaction, are all functions of the permeability of concrete. It is important to ensure that the concrete surrounding the embedded concrete has the ability to protect the reinforcing steel from corrosion. The major factor that should be considered in designing a corrosion resistant concrete is the water-cementitious ratio, which governs the permeability of concrete. The cement/material specification also plays a significant role in determining the permeability of the concrete.

A number of tests can be carried out to investigate the nature and extent and behavior of corrosion activity in concrete subjected to severe environments. Some of these tests include acid-chloride content (ASTM C1152); measures the chloride content in concrete, Polarization resistance (ASTM G59); measures corrosion rates, electrochemical impedance spectroscopy (ASTM G106); measures concrete resistivity, Chloride diffusion (ASTM C1556); measures relative diffusion rates of chlorides. This research will only focus on studying the effect that admixtures, such as SDA, may have on the corrosion behavior of concrete. This study was conducted in accordance with ASTM G109 and reference made to ASTM C876 will illustrate the probability of the formation of corrosion cells on the reinforcing steel (ASTM C876).

There has been a lot of research done on mitigating corrosion through increased concrete coverage, use of admixtures, reduced permeability concrete, migrating corrosion inhibitors, and replacement of steel rebar with alternative materials (Sharp 2004).

2.3 Cement

Cement is composed of free lime and siliceous and aluminous materials (pozzolans), which in the presence of water will chemically react with the calcium hydroxide released by the hydration process to form a cementitious paste that binds the inert materials in the concrete (ASTM C125). It is manufactured industrially by heating a homogeneous mixture of limestone and clay materials in a kiln at a temperature of 2642 degrees Fahrenheit (Bye 1999).

The most commonly produced and utilized pozzolan/cement is portland cement (Bye 1999). It is categorized (ASTM C150) into five types, I-IV, depending on the ratios of the material compositions in the cement. The different types of cement have been formulated to offer slightly different characteristics. For example, Type III is formulated to have improved early strength gain.

2.3.1 Cement versus Fly Ash

Unlike cement, which is a manufactured product, fly ash is a waste product of coal-based energy production. Both cement and fly ash exhibit similar reaction compounds and characteristics but differ in the amounts of their constituents. The compounds in portland cement, in the presence of water, will react to form calcium silicate hydrate gel (C-S-H) or calcium aluminate hydrate gel (both cementitious material), which bind the inert materials together (Neville 2006).

The standard cement hydration reaction equation is given by the following (Neville 2006):

When fly ash is incorporated in the concrete matrix above, the lime produced will react with the pozzolanic compounds present in the fly ash to produce the same C-S-H compounds formed by the hydration of cement.

The pozzolanic reactions involving fly ash vary considerably with the type of ash used. The silica content and the calcium oxide present in the fly ash will determine how much fly ash reacts in the matrix. The pozzolanic activity of the fly ash is also dependent on other parameters, such as its unburned carbon content and its fineness (Joshi and Lohtia 1997). The amorphous amino-silica compounds in the fly ash

will further react with the free lime, over time, to form more C-S-H bonds/gel. Over time, the fly ash/portland cement matrix will produce more C-S-H gel than that produced by portland cement alone hence providing additional cementitious products that impart additional strength to the concrete.

Fly Ash + Lime = (more) C-S-H

Generally, pozzolans such as fly ash, in the presence of water, will react in a similar hydration reaction as portland cement. Fly ashes containing high amounts of lime, such as the Class C type, are capable of setting independently when mixed with water, hence making it self-cementing (Berry *et al.* 2009).

Fly Ash + Water = C-S-H + (Free) Lime

Its independent use is generally not recommended because the pozzolanic reactions are much slower than the cement hydration reactions and would significantly affect the early strength and rate of strength gain significantly.

2.4 Spray Dryer Ash

Spray dryer ash is a residual material of coal-based energy production, obtained from the flue gas desulfurization process (FGD), commonly referred to as 'scrubbing.' This process removes sulfur dioxide from power plant emissions and is accomplished by adding calcium hydroxide (lime) to the flue gases (contaminated with sulfur dioxide), while at the same time the heat of the flue gases assists in drying the reaction products (Babcook *et al.* 1978). These products later collect with the fly ash produced and form a unique material that has been termed as SDA.

Dry Reaction Products + Fly Ash = Spray Dryer Ash

The fly ash is produced from burning pulverized coal in a coal-fired boiler furnace. The fine-grained waste product produced is then carried off in the flue gas and is collected from the flue gas using electrostatic precipitators (bag houses) or mechanical collection devices (cyclones). About 30%-80% of all the ash produced leaves the furnace as fly ash, depending on the boiler furnace used in the energy production (Babcook *et al.* 1978). The general flow of the process resulting in fly ash is illustrated in the following graphic.

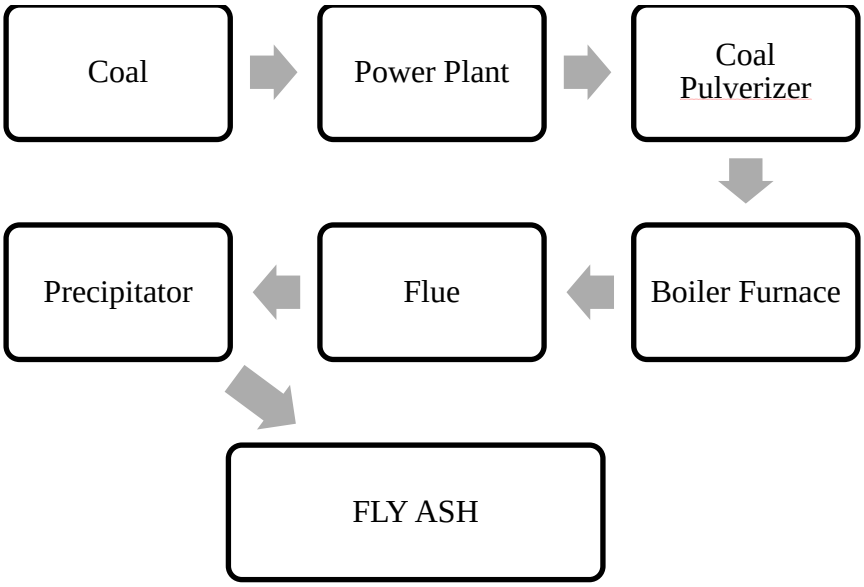

Because SDA is collected together with fly ash, it is similar to fly ash in many ways and most closely resembles Class C fly ash, which is predominant in the mid-west and western regions of the United States. It is a relatively new product, and limited research has been done on its application. The present research is based on the hypothesis that it will perform similarly to Class C ashes, therefore the following sections will address content on fly ash used in concrete, which will be used for comparison with SDA characteristics.

2.4.1 Types of Fly Ash

Several types of fly ash exist, all dependent on the type of coal and the coal combustion process, which determine the chemical composition of the fly ash. The different types vary mainly in the amount of calcium, silica, alumina, and iron they contain.

These have been classified (ASTM C618) into two basic classes:

Class F: This is obtained from burning anthracite and bituminous coal. This fly ash contains less than 10% lime (CaO), hence requires a supplemental cementing agent such as portland cement, quicklime, or hydrated lime in order to react efficiently (King 2005). When Class F fly ash is subjected to a highly alkaline environment such as sodium hydroxide or sodium silicate, a new material known as a geo-polymer is formed (Tempest *et al.* 2009).

Class C: This fly ash is obtained from burning younger lignite and sub-bituminous coal. It exhibits self-cementing properties because it contains a higher content of lime, more than 10% (King 2005). Unlike Class F, Class C fly ash does not require an activator since it contains higher amounts of alkali (King 2005).

Based on its chemical composition, the spray dryer ash being used in this research would ideally be categorized as a Class C fly ash except for its high sulfur content (>6%).

Table 2.2 compares the ASTM requirements for the different types of fly ash.

Table 2.2 Fly Ash Classification as per ASTM C618

Component	Moisture	SiO_2	Al_2O_3	Fe_2O_3	SO_3	LOI
	max. %	min. %			max. %	max. %
Class F	3	70			5	6
Class C	3	50			5	6

2.4.2 Properties of Fly Ash

Fly ash obtained from different coal plants is highly variable in its properties and is dependent on the coal combustion process that was used. Hence, fly ash is usually defined in terms of its chemical and physical properties. The most essential properties that affect the fly ash's reactivity include its fineness and loss on ignition (LOI) (King 2005).

The loss on ignition (LOI) is a measure of the unburned carbon content in the fly ash, and it greatly influences the chemical characteristics of the fly ash. The carbon content (LOI) present in the fly ash can be approximated physically by observing the color of the fly ash. The color varies from gray (Class C) to black (Class F). The lighter the color, the lower the carbon content or unburned carbon (Joshi and Lohtia 1997). The ASTM C618 specification limits the LOI to a range of 3%-6%. Fly ash containing larger amounts of unburned carbon reduces the effectiveness of air entrainers and decrease the workability of the concrete, hence impairing reactivity and strength development. Higher water content and more air entrainer is required to maintain the required workability and air content (Joshi and Lohtia 1997).

The fineness of fly ash is a key property in determining its reactivity and strength characteristics. The fine particle size reduces the porosity of the concrete and increases the volume-to-surface area ratio, which is needed for the pozzolanic reaction. The fineness of the fly ash, however, does affect the amount of air entrained in the concrete. It will increase the demand for the air entrainer needed to provide a target air content. All fly ashes have a particle size less than 0.075 mm and are mostly amorphous in nature. Class C type fly ash is generally coarser than Class F fly ash. The specific gravity usually ranges between 2.1 and 3.0. Increased particle fineness has been shown to increase the pozzolanic activity of the fly ash (Joshi and Lohtia 1997).

The proportions of the chemical constituents present in fly ash define the type of fly ash and determine the extent of its pozzolanic activity. Sufficient amounts of silica (SiO_2), alumina (Al_2O_3) and iron oxide (Fe_2O_3) are needed to react with lime, in the presence of water. The sum of these oxides must reach the required minimum of 50% for Class C and 70% for Class F. Calcium oxide (CaO) is another significant oxide that affects the pozzolanic activity of the fly ash. It governs the performance of the fly ash in concrete, which is influenced by the amorphous nature of the fly ash and is responsible for the creation of reactive (free) lime. Sulfur trioxide (SO_3) is another oxide that great affects the early strength development of the fly ash. The higher the sulfate content, the higher the resultant strength. A maximum of 5% is permissible in the fly ash to avoid excess sulfates that may contribute to disruptive sulfate attacks (King 2005).

The above physical and chemical properties of fly ash do provide improved workability, reduced permeability, increased ultimate strength, reduced bleeding, improved surface finish, and reduced heat of hydration when a fly ash-cement matrix is used in concrete (Joshi and Lohtia 1997).

2.4.3 Utilization of Fly Ash

Fly ash has been used in several engineering applications such as structural fill, waste stabilization and solidification, soil stabilization, aggregate and filler material, road sub-base, raw feed for cement clinkers, production of geo-polymer materials, mine reclamation, grout, and as partial replacement/substitution of cement (Joshi and Lohtia 1997). However, the amount of fly ash produced is still much greater than the amount of fly ash that is put to beneficial use. Millions of tons of coal combustion products are produced annually but less than 43% of the products are used beneficially. Utilization of fly ash in concrete offers environmental and cost benefits by reducing the demand for virgin materials and minerals that are used in the manufacture of cement, the amount of carbon dioxide released in the atmosphere through the cement manufacture process, and the amount of coal ash disposed of in landfills (ACAA *n.d.*). Table 2.3 illustrates the utilization of coal ash (CCP) in the recent past.

Table 2.3 CCP and Fly Ash Produced/Re-used (millions of tons) (ACAA 2010)

	CCP produced	CCP re-used	Fly Ash produced	Fly Ash re-used	Percentage re-used
2006	125	54.2	72.4	32.4	45%
2007	131	56	71.7	31.6	44%
2008	136	60.6	72.5	30.1	42%

These statistics indicate an increasing fly ash disposal challenge that requires an efficient solution. The concrete industry seeks to contribute to the solution by utilizing fly ash in its applications. One incentive for utilizing fly ash in amounts greater than 25% is that it would classify the concrete a LEED certified product (PCA 2009).

2.5 Fly Ash Concrete

Fly ash mixed with concrete has shown results of increased strength and durability of the concrete. Its utilization in the United States stretches back to 1929 when it was first used on the Hoover Dam (Smith 2006). Concrete with fly ash can be produced to achieve desired strengths at various ages, with a given water-cementitious ratio, aggregate size, air content, and slump. Concrete with fly ash has been widely used in the highway industry. Much of it is air entrained since the fineness of the fly ash provides a challenge for the concrete to maintain sufficient air voids needed for the freeze-thaw cycles (Joshi and Lohtia 1997).

In some instances, 100% fly ash (Class C) concrete has been produced and has been found to meet acceptable concrete standards. It has been used on a number of projects that entailed the construction of foundation walls and footings, floor slabs, and manufacture of precast panels. However, its use has not yet found acceptance in the construction industry due to its highly sensitive handling and quality control, and challenges experienced in adhering to the specified batching procedures. The order in which the materials are introduced into the mixture and the duration of the mixing process is of vital importance in ensuring proper setting of the concrete (Berry *et al.* 2009).

Fly ash concrete has been acknowledged as a ‘green’ product. Some states, such as California, have recognized the benefits of fly ash concrete. California’s Department of Transportation (Caltrans) requires all highway projects to use fly ash to blend all concretes (Maggenti 2009).

2.5.1 Fly Ash and Concrete Strength

Concrete strength, defined by its compressive strength, is affected/determined by a number of factors such as the water-cementitious ratio, setting time, workability, curing and pozzolanic activity − dependent on the type of pozzolan used. For example, utilization of fast setting cement will reduce the setting time and provide for its early strength development. Other pozzolans, in addition to fly ash, have been used and have provided enhanced properties and added benefits in concrete.

The effects of fly ash (both Class C and Class F) can be recognized with as little as 20% fly ash replacement of cement in the concrete. This amount can increase the setting time of concrete by about one to two hours, and doubling this amount could further increase both initial and final setting times (Joshi and Lohtia 1997). Several studies have been done to investigate the influence fly ash has on the strength (early and ultimate) of concrete, but few studies have been done with SDA. Hence, guidelines for the usage of fly ash (and its derivatives, SDA) are limited to Class C and Class F types. The ACI guidelines limit the use of Class F fly ash to 15-25% and Class C fly ash to 20-35% (ACI 1996) replacement of cement in the concrete.

Crouch *et al.* (2009) has made attempts to investigate a 50% usage for Class F fly ash, and their research findings indicate an increment in the ultimate strength despite a reduced early strength development in the concrete. Lower early strength development is the main setback when using Class F fly ash in concrete. Despite this limitation, its utilization in concrete could be enhanced by activating it with an alkali, which helps improve the hydration process. Such concrete could be referred to as geo-polymer/ alkali-activated concrete. In some instances, glass aggregates (recycled glass) could be used to improve the hydration process instead of alkalis. The recycled glass not only acts as filler material in the concrete but also plays a role in the strength development (Trejo *et al.* 2004).

The percentage of Class C fly ash typically used in structural concrete is 20-35% (ACI 1996) though in some instances 35-100% Class C Fly ash has been used to replace cement. In 1988, it was used to replace up to 70% of the cement in a highways project in North Dakota, and in 1989 it was used for concrete roads and parking lots (Golden *et al.* 2003). The concrete was designed for a target strength of 3500psi, and its 35-day strength was found to have exceeded the target.

Berry *et al.* (2009), in their research confirmed that concrete using only Class C fly ash as the cementing agent can exhibit outstanding performance in terms of compressive strength behavior. Early strength gains, in excess of 4000 psi (27.6MPa) were achieved and strength of more than 8000 psi (55.2MPa) was attained after 84 days. Its application is witnessed on the Orchard Gardens (2005)[5], a $6.5 million project that utilized 100% Class C fly ash in the community barn foundations and 35% Class C fly ash in the rest of the foundations. Kumar *et al.* (2007) also found that 50-60% Class C fly ash replacement was adequate to meet the strength requirements for concrete pavements.

Class C fly ash has an accelerated rate of chemical reaction when water is added due to the high calcium content. At elevated curing temperatures, the setting times could be reduced and an increase in the early strength development would be attained. On the other hand, the long-term strength and durability of concrete cured at elevated temperatures is still suspect (Elsageer *et al.* 2009).

[5] Orchard Gardens, http://www.greencommunitiesonline.com

2.5.2 Fly Ash and Concrete Bond Strength

Bond strength is a measure of interaction between the steel rebar and the concrete in terms of direct shear. When loaded, the concrete surrounding the rebar induces stresses onto the rebar's lateral surface, creating shear/bond stresses along the bar. It is an important structural design property that is significant to the effectiveness of the steel reinforcement in concrete and enables for the proper design and performance of reinforced concrete. Structures, concrete pavements, and bridges are designed based on the interactive behavior of the rebar with the concrete (Tonias 2007).

Strength of concrete is of paramount importance in determining the effective performance of the structure and should not be compromised by the presence of a weak bond. Over the years, research has been done addressing this challenge, and some attempts have been made to enhance the properties of the concrete by utilizing energy efficient materials such as fly ash.

Considering the smaller particle size of the fly ash (and SDA), it is presumable that utilization of fly ash in concrete would provide greater shear bond with the rebar. A number of studies carried out, though, indicate relative bond strength produced with fly ash use. Chang *et al.* (2009) investigated the shear bond behavior of fly ash based geo-polymer concrete beams and discovered that the bond strength was closely related to that of normal concrete beams. Cross *et al.* (2005) had a similar finding that showed the specimen containing 100% fly ash performed similarly to the plain reinforced concrete.

Experimental assessment of the bond strength of concrete has mainly used the conventional pull-out test (ASTM A944) to investigate the strength. Other test methods such as the direct tension pull-out test method and the beam-splice test method have also been used as alternatives or for comparison purposes.

2.5.3 Fly Ash, Durability and Rebar Protection

Durability and corrosion of the reinforcement in concrete are closely linked since failure of one would inherently affect the other. For example, the wearing out of the concrete cover would expose the rebar to the atmosphere and lead to corrosion. Durability of concrete is defined as the ability to withstand chemical attack (chlorides, sulfates, and other corrosive materials), weathering action (frost, rain, and high humidity) and abrasion while maintaining its desired engineering properties (PCA 2002). Corrosion, on the other hand, is the oxidation/rusting of the rebar caused by the ingress of water or chemicals (such as chlorides, sulfates, and carbonates) onto the rebar embedded within the concrete (PCA 2002).

Concrete utilized for pavement construction is usually exposed to inclement conditions and is very susceptible to deterioration. It is important to protect the embedded rebar and design the concrete to be able to withstand severe environmental conditions, for a long time, without significant deterioration. Freeze-thaw and steel corrosion properties of concrete are vital concerns in the maintenance and longevity of transportation infrastructure and, therefore, help define the scope for this report.

In addition to providing a sufficient concrete cover, innovative methods/designs should be introduced to make concrete more resistant to attack and less porous to any ingression. Previous studies show that the utilization of fly ash in concrete provides improved impermeability within the concrete, though other chemical effects could cause its deterioration. In his thesis, Burden studied the effects of curing on the carbonation and permeability of high volumes of Class C and Class F fly ashes and discovered that the rate of carbonation increased and permeability decreased over time with an increment in the amount of fly ash used (Burden 2006). He suggested that carbonation-induced corrosion could be offset by extending the moist curing time and increasing the concrete cover.

When not exposed to any chemical environment, fly ash concrete serves as a very durable material since its water permeability and void content are reduced with an increase in fly ash used (Crouch *et al.* 2009). This is due to the pore refinement that is provided by the fineness of the fly ash. The fly ash concrete matrix also reduces the permeability to chlorides, and sulfates and carbon dioxide penetration in concrete, hence reducing corrosion of reinforcement bars embedded within and improving the durability of the concrete (Joshi and Lohtia 1997).

In the past century, a new method was introduced to make concrete exposed to freeze-thaw conditions more resistant. Air entrainment admixtures were created and are presently being incorporated into transportation concretes. The introduction of the admixtures produces small air bubbles, which allows for flexibility in the freeze-thaw cycles that the concrete would be subjected to. Similar to the admixtures, the use of fly ash has been observed to produce durable concrete. The utilization of the combination of fly ash and air entrainment is observed to enhance the freeze-thaw durability of the concrete as long as the carbon content of the fly ash is within a 6% limit (Russell *et al.* 2006).

3. EXPERIMENTAL SET-UP

In this study, four sets of experiments were conducted to characterize the overall performance of the SDA concrete. Varying amounts of SDA are used as a replacement of cement (binder) in the concrete mixes used to manufacture the test specimens. Several design mixes are tested for their compressive strength, each tested at 3, 7, 14, 28, and 56 days. Mixes were also prepared and tested in accordance to the appropriate ASTM standards to determine bond strength (A944), corrosion related (G109 and C1152) and durability/ freeze-thaw (C666) properties of the concrete.

3.1 Materials

3.1.1 Spray Dryer Ash

The SDA used in this research was obtained in Northern Colorado at the Rawhide Power Station, managed by the Platte River Power Authority. The specific gravity of the SDA used is 2.71 g/cc. This SDA has a significant amount of lime at 23.65% and a sulfur trioxide content of 6.19%, which exceeds the ASTM C618 limits for Class C fly ashes for use in concrete, as shown in Table 3.1. The increased lime (in addition to the lime content in the Class C fly ash) and sulfur contents are contributed by the scrubber process.

Table 3.1 Partial Chemical Composition of the Spray Dryer Ash (SDA) Used[6]

	SiO_2	Al_2O_3	Fe_2O_3	CaO	SO_3	LOI
SDA Composition (%)	39.76	14.31	5.56	23.45	6.19	1.65
ASTM requirement for Class C (%)	Total >50			-	<5.0	<6.0

3.1.2 Other Materials

Type I/II cement conforming to ASTM C150 “Standard Specification for Portland Cement” is used to manufacture test specimens. The aggregates meet ASTM C33 “Standard Specifications for Concrete Aggregates.” Well-graded, normal weight aggregates are used as coarse aggregates and natural sand for fine aggregates. The material specifications are indicated in Table 3.2.

Table 3.2 Concrete Material Specifications

Constituent Material	Description	Specific Gravity	Moisture Content (%)	Bulk Unit Wt	Fineness Modulus
Cement	Type I/II (ASTM C150)	3.15	NA	NA	NA
Coarse Aggregate	Well-graded, 3/4" max. size	2.68	2.00	-	NA
Fine Aggregate	Natural sand (ASTM C33)	2.64	1.00	-	2.80

‘Micro-Air™’ air entraining admixture (a BASF product) is used to make specimens for freeze-thaw testing and conforms to the specifications of ASTM C260 “Standard Specification for Air Entraining

[6] SGS North America, Inc.

admixtures for Concrete." The admixture is an aqueous solution of alkyl aryl sulfonate, which is added to the water used for concrete mixing.

3.2 Mix Design

The PCA Absolute Volume method (Komastka *et al*. 2002, Appendix A, Table 3.3) is used to design the concrete mixes, with the constituent materials previously described (Table 3.2). The absolute volume method computes the absolute volumes of the constituent concrete materials using the parameters given in Tables 3.2 and 3.3 and later converts the volumes to weights (Tables 3.4 and 3.5) through the use of the individual specific gravities.

The mix design is based on a Class S35, a dense high strength structural concrete that is specified by CDOT for higher strength concrete and is normally utilized for bridge deck construction (CDOT 2008). The concrete mixes are standardized against the Class S35 standard concrete mix design for a strength of 4500 psi (31MPa). To ensure that the desired strength of 4500 psi is met, the PCA method bases the actual design on the target (required mean) strength, which accounts for any irregularities or flaws that may occur in the concrete preparation process.

Table 3.3 Summary of the PCA Absolute Volume Method for a Cubic Yard (27 ft^3)

	Non-Air Entrained Concrete	**Air Entrained Concrete**	**Units**
Desired compressive strength	4500	4500	psi
Target compressive strength	5700	5700	psi
Water/cementitious ratio	0.525	0.440	-
Air content	2	5	%
Slump desired	1	1	in
Water content	5.45	4.90	ft^3
Cementitious content	3.30	3.53	ft^3
Coarse aggregate content	10.03	10.03	ft^3
Fine aggregate content	7.70	7.20	ft^3

The mixes used for the compressive and bond strength tests are non-air entrained while the durability (freeze-thaw) and corrosion test mixes are air entrained. The details for the mixes used for the different types of tests are shown within the test descriptions.

3.3 Compressive Strength Test

The concrete for the compressive strength tests was designed using the PCA absolute volume method for a design strength of 4500 psi (31MPa) with a target strength (at 28 days) of 5700 psi (39MPa) and a slump ranging between 1"-3" (25-75 mm), hence a water/cementitious ratio of 0.525 is used. The concrete mixes were made using Type I/II cement that conforms to ASTM C150 and without the use of any water reducers. They are prepared and batched by weight with varying percentages of SDA added to replace varying percentages of the cement and fine aggregates, as shown in Table 3.4.

Table 3.4 Non-Air Entrained Concrete Mixes; Design Strength 4500psi /31MPa

Parameter	Control	Mix 1	Mix 2	Mix 3	Mix 4	Mix 5	Mix 6	Mix 7	Mix 8
SDA (%)	0	15	20	25	30	35	40	45	50
Water (lb)	324	324	324	324	323	323	323	323	323
Cement (lb)	648	550	518	486	453	421	389	356	324
SDA (lb)	0	97	130	162	194	227	259	291	324
Coarse agg (lb)	1707	1707	1707	1707	1707	1707	1707	1707	1707
Fine agg (lb)	1279	1265	1261	1256	1252	1248	1243	1239	1234

The concrete is prepared according to ASTM C192 "Standard Practice for Making and Curing Concrete Test Specimens in the Laboratory." Both metal and plastic cylindrical molds were used to cast cylinders and a small concrete mixer was used to manufacture the concrete. Three cylinders were manufactured for each point required to be tested. The concrete samples were moist cured at a 99% humidity level and each cylinder specimen was tested to failure using a compression tester (Figure 3.2) with a loading rate of approximately 30.4 psi/sec (212 KPa/sec) after 3, 7, 14, 28, and 56 days of curing. The results of the three cylinder tests are averaged for each point and tabulated. Results are discussed in Section 4.

Figure 3.1 Compression Testing Machine

3.4 Bond Strength Test

Bond strength tests were conducted at the Engineering Research Center, in accordance to ASTM A944 – 05 "Standard Test Method for Comparing Bond Strength of Steel Reinforcing Bars to Concrete using Beam-end Specimens." The test aims to determine the bond strength of concrete specimens containing variable amounts of SDA.

Concrete beams of 24" x 9" x 17" (610 mm x 229 mm x 432 mm) were cast in wooden forms as shown in the schematic in Figure 3.2. A No. 4 (No. 13) steel reinforcement bar was used as the main bar for the bond/anchorage strength testing. The rest of the bars played a passive role in the test, but facilitated

moving the specimens around the lab. The main rebar was placed from one end of the specimen to the halfway point of the specimen, where it was linked to a ½ in (12.5 mm) diameter hollow steel conduit by a polyvinyl chloride (PVC) bond breaker, as shown in Figure 3.2. The conduit allowed for access for displacement measurement.

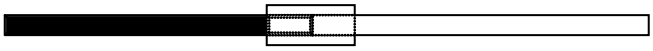

Figure 3.2 Beam/ Rebar Specimen set-up

Design mixes similar to the compressive strength test were used for the bond test. The concrete (Table 3.4) was prepared by machine mixing and was cast and compacted into the molds in three layers, using a tamping rod. A total of nine specimens were made with three of each containing 0%, 25%, and 50% SDA replacement. The specimens were moist cured at 99% humidity in a curing room for at least 28 days.

Figure 3.3 shows pictures of the actual laboratory implementation of this test. Each specimen was positioned against the yoke linked to the actuators. The rebar at one end of the beam was gripped by the wedge grip attached to the yoke, and a compression member was placed against the bottom edge of the beam. The beam was held down on the opposite end by a tie down C- section to prevent rotation of the beam specimen while the rebar was being pulled out.

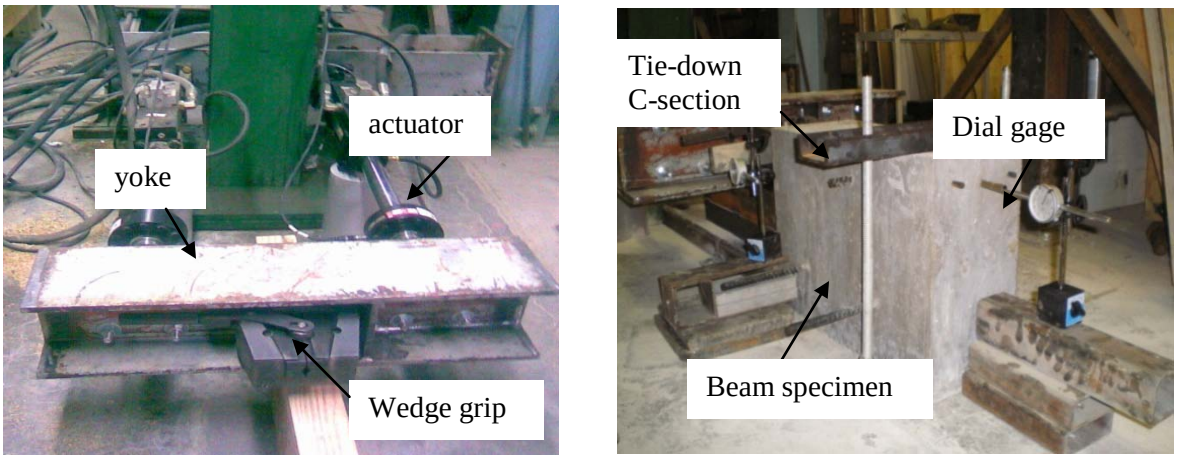

Figure 3.3 Schematic of Beam- End Specimen and Apparatus

The test method was conducted by pulling the No. 4 rebar from the concrete beam at a constant loading rate of 0.05-0.1in/min, until failure. The variation of the bond strength (force) with the displacement of the rebar was measured at the actuator by a software program, whose results correlate with the bond force present at the concrete-rebar interface. Dial gages were also attached at either end of the rebar to measure the relative displacement of the rebar as it was being pulled out of the concrete. The dial gage readings were recorded manually at 10 second intervals, in synchronization with the actuator readings.

Concrete cylindrical samples were also cast and tested for 28-day compressive strength to determine the strength of the concrete in the bond strength specimens. The results attained from the actuator's software, dial gages, and compression testing machine were recorded and results are analyzed in the successive section.

3.5 Durability (Freeze-Thaw) Test

This test's aim is to determine the relative dynamic modulus of elasticity and durability factor of the SDA concrete specimens when subjected to repeated cycles of freezing and thawing. The modulus and the durability factor are a measure of the concrete's deterioration and are a function of its fundamental transverse frequency.

Due to the repeated cycles of freezing and thawing, concrete utilized for this purpose is usually air entrained. The control concrete used in the freeze-thaw testing was designed for a similar design strength of 4500 psi (31MPa) at 28 days, but with a 5% air content. Mixes for the concrete specimens containing SDA were designed in reference to the control concrete mix, so as to allow for a comparison of the effect of cement replacement by SDA. To maintain a consistent design strength with the standard concrete utilized in the other tests, concrete containing air entraining admixture had its water/cementitious material ratio adjusted to 0.44. The mix designs are shown in Table 3.5.

Table 3.5 Air-Entrained Concrete Mixes (Design Strength 4500psi (31MPa))

Parameter	Control	Mix 1	Mix 2
SDA (%)	0	25	50
Water (lb)	305	305	305
SDA (lb)	0	173	347
Cement (lb)	693	520	347
Coarse aggregate (lb)	1708	1708	1708
Fine aggregate (lb)	1279	1256	1234
Air entrainer content (fl.oz)	19	35	52

Trial mixes were conducted to determine the dosage of air entrainment required to provide the desired 5% air content in each of the 0%, 25%, and 50% SDA concrete mixes. Varying amounts of air entrainer were added to each trial mix; a sample of the concrete was taken from each trial and was tested for the air content using the volumetric method (ASTM C173) and air indicator kit (AASHTO T196) as a confirmatory test. These methods involved the addition of isopropyl alcohol atop a sample mortar paste placed in the testing bowl (volumetair) as shown in Figure 3.4.

Figure 3.4 Air Entrainment Testing Apparatus

The test apparatus was inclined at 45°, rolled across a flat surface and shaken until all the air in the mortar paste was completely displaced by the isopropyl alcohol. The amount of air displaced was recorded as the air content of the concrete sample. This test procedure was repeated several times until an air content of 5% was obtained. The amount of air entrainer that provided the 5% air content was noted as the sufficient amount. Generally, more air-entrainer was required with increasing SDA quantities. The amount of air entrainer used ranged between 6-17 fl. oz. (177-503 ml) per 100 lbs. (45 kg) of cementitious material.

Durability testing of the mixes was conducted in accordance with ASTM C666-97 "Standard Test Method for Resistance of Concrete to Rapid Freezing and Thawing." Three concrete prisms (Figure 3.5) of 16" x 3" x 4" (406 mm x 76 mm x 102 mm) were prepared for each of the mixes containing 0%, 25%, and 50% SDA. The specimens were soaked in water contained in stainless steel containers with internal dimensions of 16.25" x 3.25" x 4.50" (413 mm x 83 mm x 114 mm), and subjected to repeated cycles of freezing and thawing in a refrigerator. The freezing and thawing cycle involved alternating the temperature of the specimen from 40 ^{o}F to 0°F (4.4-17.8^{o}C) within four hours, with half the time given to freezing and thawing respectively.

Figure 3.5 Concrete Prisms for Freeze-thaw Testing

After each set of 35 cycles, the specimens were weighed and tested for the fundamental transverse frequency (ASTM 215) using an accelerometer linked between the specimen and a frequency analyzer as shown in Figures 3.6 and 3.7.

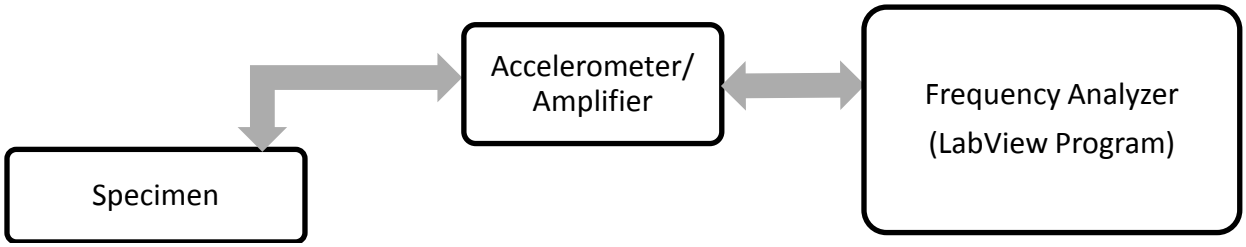

Figure 3.6 Schematic of Apparatus for Transverse Frequency Test

Figure 3.7 Picture of Apparatus for Frequency Testing

The specimen beng tested was placed on soft rubber supports, and an accelerometer was attached onto the top edge of the specimen. An impact hammer, designed to the standard specifications (ASTM C215), was used to strike the center of the specimen to induce vibrations within the specimen. The vibrations were picked up and measured by the accelerometer and recorded using a frequency analyzer, which is a program written using LabView software (Figure 3.8). The program recorded at least 5000 points of the frequency waveform per iteration, and the peak frequency was recorded as the transverse frequency of the concrete specimen. Several iterations/strikes were made and results averaged for each specimen.

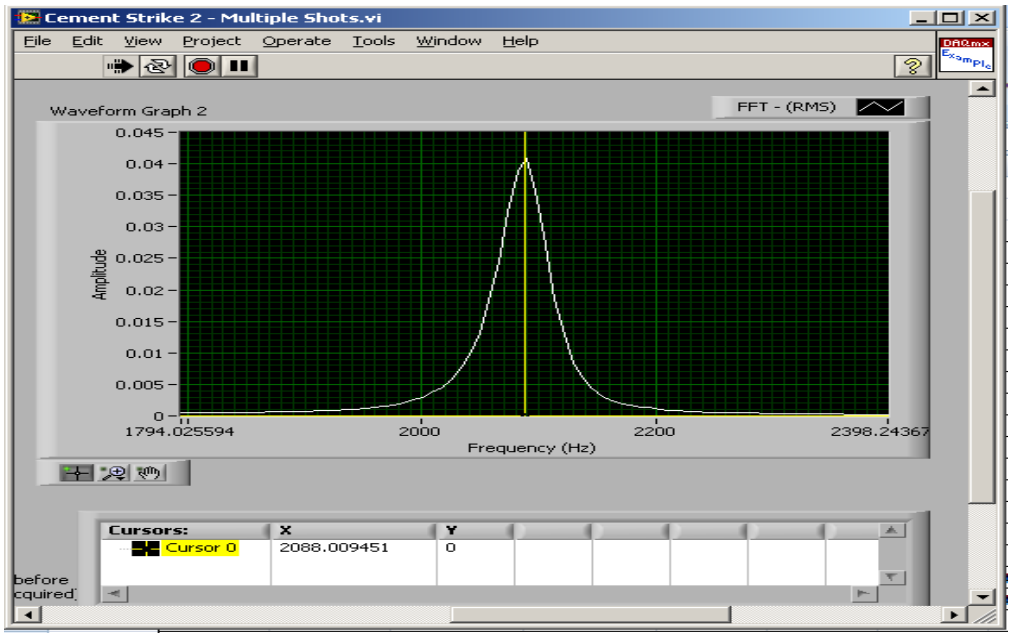

Figure 3.8 LabView Program

The results were tabulated and used to determine the relative dynamic modulus of elasticity and the durability factor. The relative dynamic modulus of elasticity (RDM) is determined through its relationship to the concrete specimens' transverse frequencies (n_c) at varying numbers of cycles (c) against its initial transverse frequency (n), as shown in equation 3.1.

$$RDM = \frac{n_c^2}{n^2} \text{ x } 100 \tag{3.1}$$

While the durability factor (3.2) is determined through its relationship with the RDM, number of cycles at which RDM reaches the specified minimum value for discontinuing the test (N) or the specified number of cycles at which the exposure is to be terminated (whichever is less) and the specified number of cycles at which the exposure is to be terminated (M).

$$DF = \frac{(\mathrm{RDM})\mathrm{N}}{\mathrm{M}} \tag{3.2}$$

The test, conducted in accordance to ASTM C 666, was terminated after 300 cycles of repeated freezing and thawing exposures, since none of the specimen's RDM dropped below 60% of its initial modulus.

3.6 Corrosion Tests

The aim of these tests is to investigate the corrosion inhibition or acceleration properties of concrete with SDA used as a binding agent and to evaluate its effect on the corrosion of steel in concrete. First, specimens were prepared and cast in reference to ASTM G109 "Standard Test Method for Determining the Effects of Chemical Admixtures on the Corrosion of Embedded Steel Reinforcement in Concrete Exposed to Chloride Environments."

The rebar required for the testing were prepared by power brushing to near white, and then later soaked in hexane to clean them. They were allowed to dry. One end of the rebar was drilled and tapped to make provision for contact screws and nuts. Both ends of the rebar were taped with electroplater tape and with neoprene tubing, exposing 8 in (203 mm) within the middle portion. The ends of the tubing were filled with two-part epoxy. The rebar specimens were then placed in the timber forms as shown in Figure 3.9 with each specimen containing two bars placed at the bottom and one positioned at the top.

Figure 3.9 Timber Forms and Rebar for Corrosion Specimens

Air-entrained concrete designed to meet 4500 psi (31MPa) strength at 28 days (Table 3.5) was prepared and cast in the timber forms. The concrete specimens were later moist cured for at least 28 days. On removal from the curing room, the specimens were allowed to dry before 3" x 6" x 3" (76 mm x 152 mm x 76 mm) plastic (Acrylic) dams were glued with silicone caulk onto the top surface. Epoxy was later applied to the concrete on all four sides and top surface outside the dam (Figure 3.10b).

Figure 3.10 a) Corrosion Specimens b) with Plastic dams and Epoxy

The specimens were then supported on half-inch non-conducting supports, soaked in a 3% sodium chloride (salt) solution at a depth of half-inch and stored at 50% humidity. The plastic dams were also half filled with 3% sodium chloride (NaCl) solution.

The specimens were soaked for 14 days in the NaCl solution, after which they were removed and allowed to dry for another 14 days. At the end of the drying period, the total potential (*TC*) and voltage (*V*) across the 100-Ω resistor (between the top and bottom rebars) was measured and used to compute the macrocell current (i*)*, which is given in equation (3.3).

$$i = \frac{V}{100} \tag{3.3}$$

The total corrosion (corrosion potential) of the rebars was measured against a silver nitrate ($AgNO_3$) reference electrode (ASTM C876) placed in the plastic dam on top of each specimen measured. The corrosion potential (*TC*) is measured in Coulombs and is given in equation (3.4).

$$TC_j = TC_{j-1} + [(t_j - t_{j-1}) * (i_j + i_{j-1})/2] \tag{3.4}$$

The specimens were then re-subjected to the same cycle of soaking and drying for a total of five months. At the conclusion of the electric potential testing, concrete samples were collected from the test specimens and ASTM C1152 was used to determine the concentration of acid soluble chlorides at three different depths in the specimens. The acid soluble chloride content is equal to the total chloride in most circumstances (ASTM C1152). Samples of the concrete were collected using a concrete drill. The drill was operated to a depth of approximately 1.5 in. (38 mm) to collect the "top" sample, to a depth of approximately 3 in. (76 mm) to collect the "center" sample, and a depth of approximately 4.5 in. to collect the "bottom" sample. The powered concrete was stored in air-tight plastic containers until titration testing was conducted.

To prepare the solution for titration, 10 g of ground concrete was placed in a beaker with 75 mL of water and 25mL of dilute nitric acid. The mixture was stirred with a glass rod. The standard called for the addition of three drops of methyl orange indicator, but three drops did not produce the desired color change, thus fifteen drops of methyl orange indicator were added to the beaker. Additional nitric acid was added until a pink color persisted. The beaker was covered and heated to boiling. The solution was filtered through coarse-textured filter paper and allowed to cool to room temperature. The beaker was then placed on a magnetic stirrer and 2mL of 0.05 N NaCl solution was added. A 10mL buret filled with 0.05 N $AgNO_3$ was placed above the solution, and the solution was gradually titrated with the use of a chloride selective electrode. The chloride content by percent mass of the concrete was calculated using equation (3.5), where V_1 is the volume of $AgNO_3$ used for sample titration, V_2 is the volume of $AgNO_3$ used for blank titration, *N* is the normality of the $AgNO_3$ solution, and *W* is the sample mass (10g).

$$Cl, \% = 3.545[(V_1 - V_2)N]/W$$

4. RESULTS AND ANALYSIS

4.1 Compressive Strength

Test cylinders whose cement quantities were partially replaced with SDA varying from 0-50% were cast and tested until failure as shown in Figure 4.1. The ultimate compressive strength of the test specimen at failure was noted, and raw results from each test are given in Appendix B. The results indicated in the following sub-sections are the average results for compressive strength of three-specimen samples.

Figure 4.1 Concrete Test Specimens at Failure

4.1.1 Early Strength Gain (0-7 days)

The results shown in Figure 4.2 it is apparent that the presence of SDA clearly decelerates the early strength gain (within the first three to seven days). This is probably due to the slow activity of the pozzolanic reaction occurring during the curing process. All mixes with SDA have a lower 3-day strength than the control mix. As the amount of SDA increases, the difference in strength between the SDA mixes and the control mix also increases. Approximately a 10% reduction in the strength is observed for samples with small amounts of SDA replacement within the first three days. Larger reductions of approximately 50% were observed for the larger SDA contents.

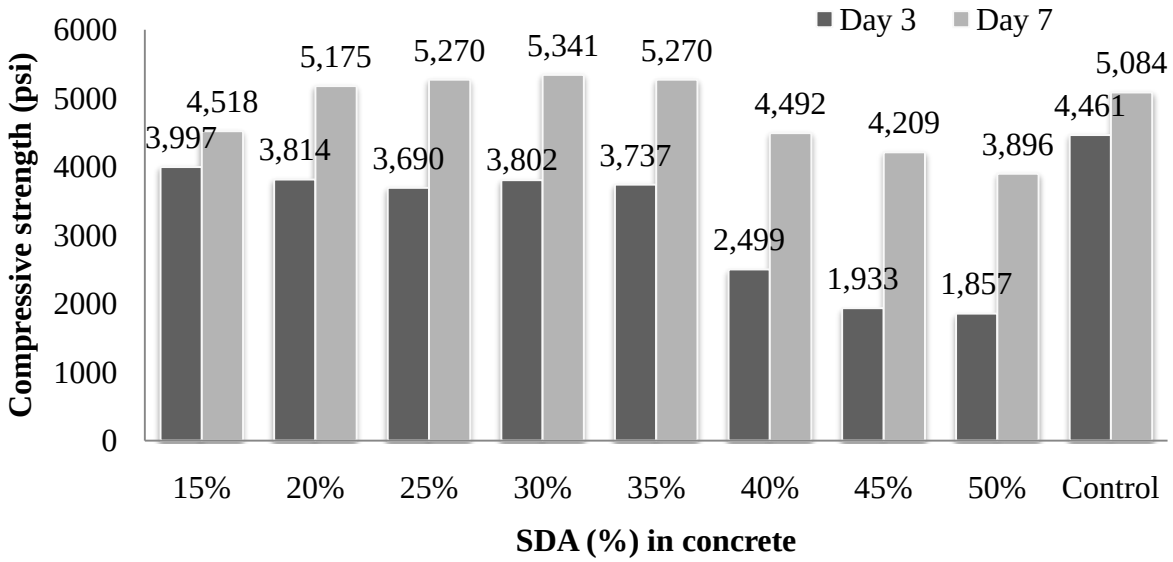

Figure 4.2 Early Compressive Strength of SDA Concrete

Within the next four days, an increase in the concrete strength in excess of the 5084 psi (35MPa) achieved by the control mix is observed for specimens with SDA varying between 20-35%. Beyond 35% cement replacement by SDA, the strength gained at seven days of curing is much lower than the control.

4.1.2 Rate of Strength Gain

Concrete with SDA exhibits an initial low strength development (within the first seven days) but later gains strength steadily. Generally, an increase in the rate of strength gain is observed at later stages in the curing process (beyond seven days of curing) when increasing quantities of SDA are added to the concrete as compared to standard (control) concrete (Figure 4.3). The trends in the results indicate that all specimens attained about 70-80% of their 28-day strength within the first seven days of curing. Beyond the seven days, specimens containing SDA had their strength increase steadily until they exceeded the target strength of 5700 psi (39MPa) at 28 days. At 56 days of curing, all specimens with SDA varying between 20-50% had a strength exceeding that of the control specimen by about 2-16%.

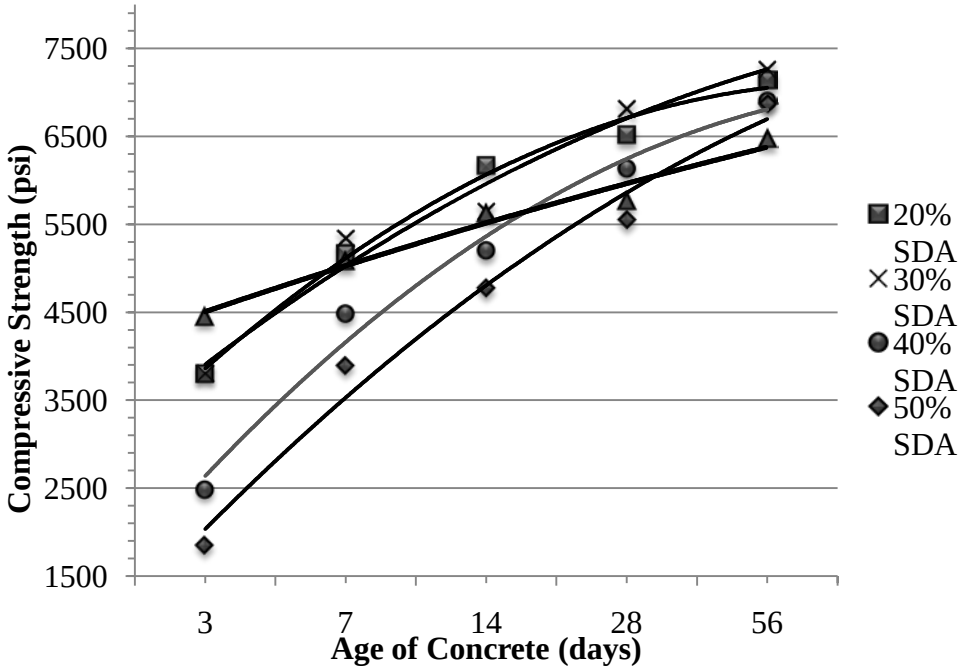

Figure 4.3 Compressive Strength Against Age of Concrete

4.1.3 Ultimate Strength

The ultimate compressive strength of concrete is usually assessed by its 28-day strength, though with fly ash mixes, a 56-day strength has also been considered. Figure 4.4 illustrates the results for the 28-day and 56-day strength in comparison to the control concrete mix.

It can be observed that the results of the entire set of specimens are within range of the control specimens at both 28 and 56 days of curing. Specimens with SDA of 15% and 50% have a lower 28-day strength gain than the control mix, though the magnitude of the difference is not significant compared to the target design strength of 5700 psi. The strength of the rest of the specimens, containing 20-45% SDA, did exceed the 28-day target strength and generally that of the control specimens.

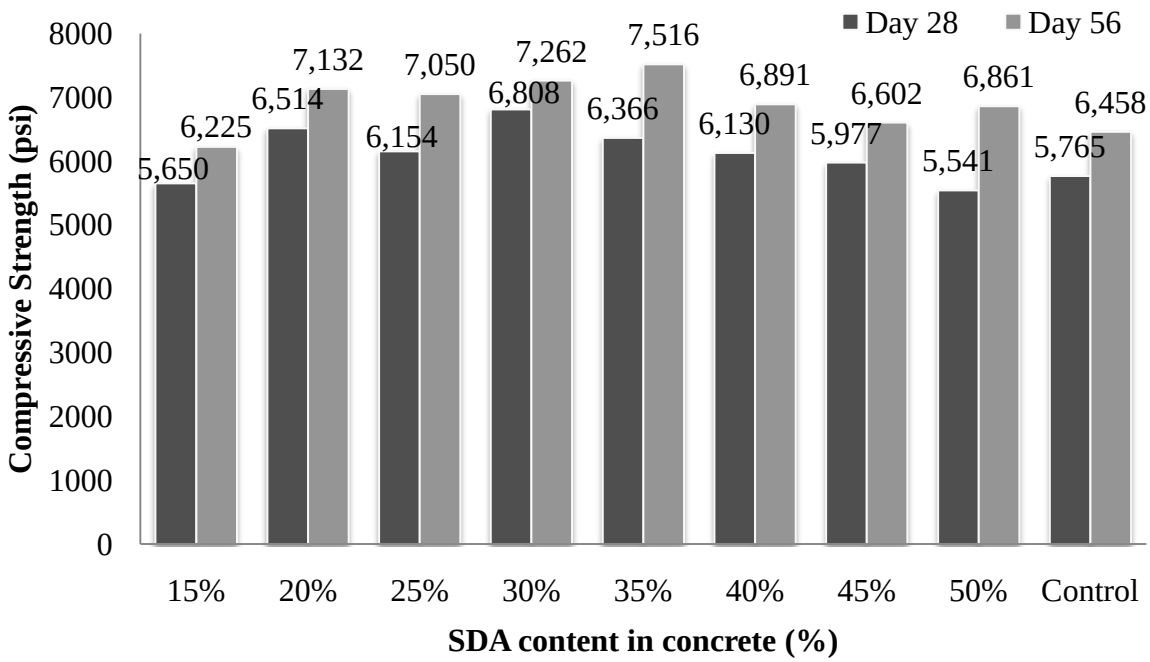

Figure 4.4 Compressive Strength Against SDA Concrete (for 28 and 56 Days)

At 56 days of curing, the strength of all specimens in excess of 20% SDA exceeds the 6458 psi (45MPa) attained by the control concrete. From the graph (Figure 4.4) it can be deduced that utilizing SDA would provide some long-term strength benefits compared to the control (standard) concrete. The SDA provides a 4-18% added benefit on ultimate strength gain of concrete at 28 days and approximately 6-15 % at 56 days.

The trends in Figure 4.4 show that concrete with SDA ranging between 25-35% provides the most favorable results for compressive strength. Beyond 35% SDA, the trends seem to indicate a reduction in the strength as more SDA is added to the concrete. It is probable that at some point beyond 50% replacement, SDA would cease to provide added benefit when utilized in concrete.
The results also verify that the range of variable mixes chosen for the compressive strength test with 10-50% SDA were viable, hence a reduced range was chosen for testing for the next three sets of tests. Due to the time constraints for the research, only three different concrete mixes were considered for experimental investigation. The chosen sample points for the rest of the tests are specimens with 0% (control), 25%, and 50% of their portland cement content replaced by SDA. The points selected were chosen to range about the recommended limits (ASTM C618) of 20-35% fly ash utilized in replacement of cement in concrete.

4.2 Concrete Shear Bond

This section presents the results for the pull-out (bond) test (ASTM A944) that was carried out to investigate the concrete-steel bond behavior in concrete specimens containing 25% and 50% SDA. The bond specimens were cast from non-air entrained concrete in wooden forms. At the same time cylinders for compressive strength tests were prepared to confirm the strength of the concrete used in the bond specimens. Both tests were conducted after a minimum of 28 days (at 35 days) of moist curing.
The results in the following sub-sections address the compressive and bond strength of concrete specimens containing 0%, 25%, and 50% SDA. The physical behavior and mode of failure of the beam specimens are discussed in the first section. The next sections quantitatively examine the bond behavior

of the specimens in terms of the displacements and strengths recorded during testing. The last section presents the results of the compressive strength tests and discuss their relationship to the bond strength.

4.2.1 Mode of Failure

The beam specimens were loaded monotonically under a pull-out test (ASTM A944), and two types of failure mechanisms were observed. These included longitudinal cracks and pull out of the steel rebar. Longitudinal cracks of similar patterns were physically observed among most of the test specimens, with the exception of two of the specimens, as reflected in Table 4.1.

One of the beam specimens with 50% SDA (B7) did not exhibit any physical failure mode despite the increase in load. This could be attributed to the ductile behavior that was uniquely exhibited in this beam (Figure 4.7). The other beam (B2) that did not display a failure mode simply did not exhibit cracks on the surface despite reaching its peak load; based on the load at failure, this beam appears to have failed prematurely.

Figure 4.5 Beam Loaded Indicating Shear Bond Failure

The cracks began to form gradually at the front of the specimen and continued to propagate up to the approximate midpoint on the top face of the specimen as the maximum load was approached (Figure 4.5). Upon failure, the initial crack widened and terminated in an inverted T, hence permitting the complete pull-out of the rebar. At this point, the behavior of the bond-slip response was nonexistent.

4.2.2 Load-Slip Response

A total of nine beams were prepared for the pull-out test and tested after 35 days of moist curing. The tests on the beams were carried out over several days and were subjected to variable loading rates. Three loading rates (0.050, 0.075, and 0.100 in/min) were used in the test. An initial loading rate of 0.050 in/min was used on the first specimen tested. The loading rate was later increased to 0.075in/min and 0.100 in/min for the rest of the specimens as illustrated in Table 4.1, since the first specimen took over 30 minutes to fail. The variable rates affected the duration at which the peak results were attained.

Table 4.1 Summary of Bond Test Results

SDA (%)	Beam Number	Loading Rate (in/min)	Peak Load (kips)	Peak Slip (in)	Description of Failure
0%	B1	0.075	17.870	0.095*	Longitudinal crack-¼way center
	B2	0.075	8.049	0.035	No visible crack
	B3	0.05	16.969	0.035	Longitudinal crack-¼way center
25%	B4	0.075	19.486	0.452	Longitudinal crack-½way center
	B5	0.075	19.511	0.418	Longitudinal crack-½way center
	B6	0.10	12.538	0.089	Longitudinal crack-¼way center
50%	B7	0.10	(20.906)**	(0.500)**	No visible crack
	B8	0.10	17.471	0.183	Longitudinal crack-½ center
	B9	0.10	19.288	0.137	Mild crack formed at center edge

*value noted does not correlate to peak load (excluded from discussion)
**no peak values – specimen results simply plateaued out (last highest value is noted)
~~BX~~ – values excluded from discussion.

The results of loads against the displacements (slip) of a No. 4 (0.5”) reinforcing steel bar are discussed in the following sections. Various displacement measurements are recorded: one by the actuator and two by the dial gages at both closed and open ends of the specimen apparatus. The load results are obtained from the actuator measurements while the (actual) slip results used for analysis are obtained by computing the difference between the dial gage readings at the closed and open end of the specimens. The computed slip results denote the actual slip of the rebar. The actuator recorded redundant slip readings, hence they could not be used to denote the actual slip, but only the peak loads. The curves generally exhibit a similar polynomial trend; the curves peak to a maximum, and later descend as expected. Beyond the peak value, there is no more concrete-steel bond relationship, and any increase in load simply pulls out the steel bar.

4.2.2.1 Specimens with 0% SDA

Figure 4.6 shows the load-displacement response of the individual specimens with 0% SDA that were tested as control specimens. The computer (actuator) measurements and dial gage readings at the closed end convey similar patterns in the load-slip behavior (Figure 4.6). The variation of the dial gage readings can be attributed to the strain occurring in the steel during pull out. Details of the strain discussion are addressed in Section 4.2.4. The dial gage readings of 4.6 (a) and (c) do not correlate well with the computer (actuator) readings due to poor synchronization of the manual and computer measurements. Therefore, the actual bond-slip behavior is assumed to compare parallel to total slip (blue curve), and an approximation of the maximum slip of 0.6 and 0.4 inches respectively is made.

Beam specimen B2 (Figure 4.6(b)) exhibits an expected trend but peaks at a much lower value than the other specimens of similar mix design. An error in the consolidation of the concrete is presumed to be the source of the poor bonding of concrete with the rebar. Hence, the beam (B2) is eliminated from the subsequent discussion of results.

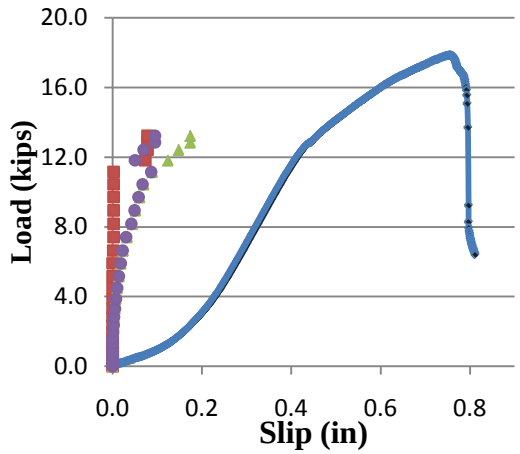

Figure 4.6(a) Load vs. Slip for Beam (B1)

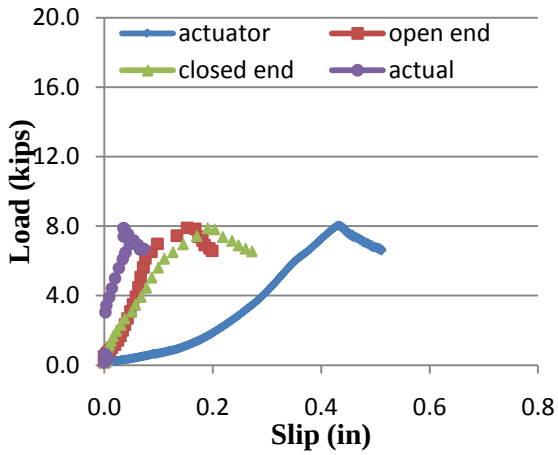

Figure 4.6(b) Load vs. Slip for Beam (B2)

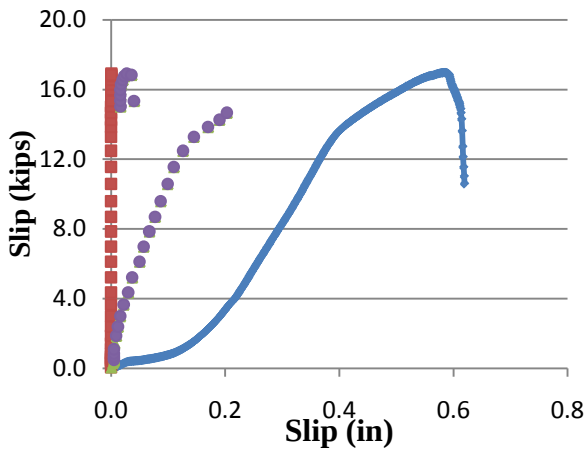

Figure 4.6(c) Load vs. Slip for Beam (B3)

4.2.2.2 Specimens with 25% SDA

Figure 4.7 illustrates the load-slip results (load results from actuator against actual slip results obtained by computing the difference between the dial gage readings at the closed and open end) for the individual specimens with 25% SDA, measured by the actuator and dial gages. Beams B4 and B5 exhibit very similar behavior and both peak at about 20 kips. Beam specimen B6 peaks at a much lower value, and this was due to slackness of the embedded steel bar in the concrete. The consolidation of this specimen is inadequate; hence, inadequate concrete bond was actualized around the rebar. Therefore, beam B6 is omitted from the discussion of the results, and only beams B4 and B5 are considered for analysis.

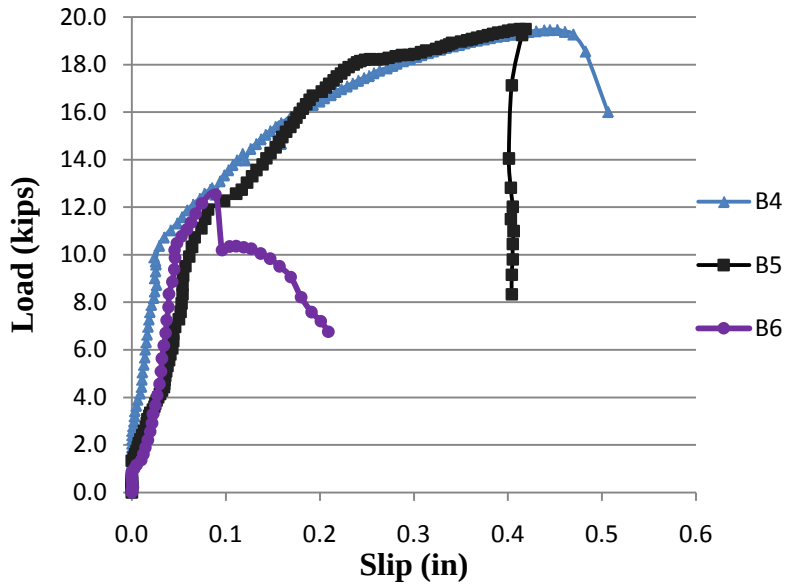

Figure 4.7 Load vs. Slip for Beams (B4, B5, B6) with 25% SDA

4.2.2.3 Specimens with 50% SDA

The beams prepared with 50% SDA exhibit very similar behavior in all three specimens with the exception noted with the peak/plateau behavior (Figure 4.8). Beam B7 exhibits an expected trend of an increase in slip with an increment in load, except that it failed to peak. The beam simply plateaus and displays very ductile behavior. The variations of the peak (plateau) values for the beams range between 17-21 kips.

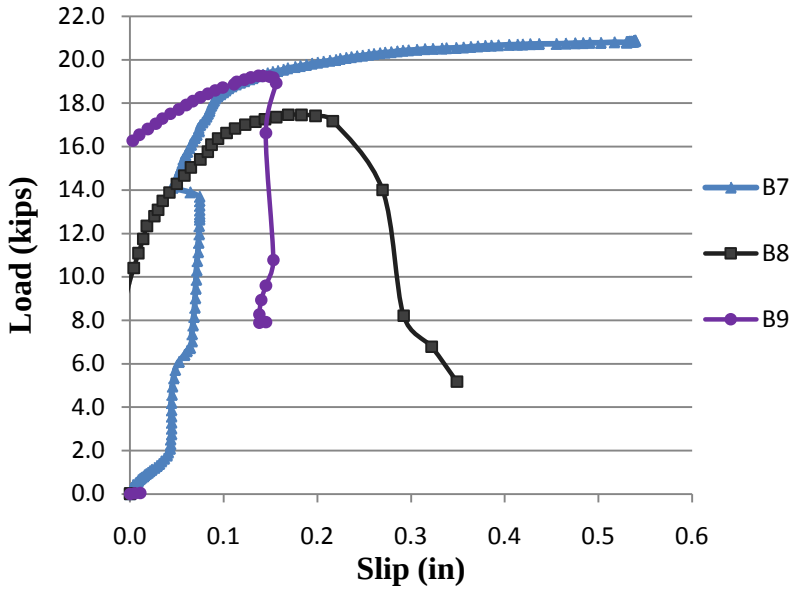

Figure 4.8 Load vs. Slip for Beams (B7, B8, B9) with 50% SDA

4.2.3 Bond Strength

The control concrete specimens portray the lowest bond strength in this experiment. Their average peak strength is the lowest at 17.420 kips, while the specimens with 25% SDA portray the highest average peak value of 19.499 as illustrated in Table 4.2. In comparison to the control, the specimen with 25% SDA exhibits the better bond-slip response.

Specimens with 50% SDA do exhibit a higher peak value than the control, though the trend of results indicates a decrease in the peak load (bond strength) with an increase in the SDA content. However, it is difficult to determine at what SDA content the peak values would start to drop below that of the control specimen. The outcome is as expected when compared with the compressive strength results in Section 4.2.5, since the bond strength is directly proportional to the compressive strength of concrete.

Table 4.2 Average Results of Peak Loads (kips), Peak Slips (in), and Rebar Strains

SDA (%)	Peak Load (kips)	Peak Slip (in)	Rebar Strain
0%	17.420	0.500*	0.0417
25%	19.499	0.435	0.0363
50%	18.380	0.160	0.0134

* approximated from curve comparison

Deducing from the results, the utilization of SDA in concrete is seen to increase the shear bond behavior of the concrete. Overall, SDA offers better bond strengths than the control specimen though the variations of 12% (25% SDA) and 5% (50% SDA) are relatively small. From the result of observation and comparison between the bond strengths, the best results are attained when SDA is utilized in concrete within limits not exceeding 25% replacement.

4.2.5 Peak Slip and Strain

As seen in Figures 4.6, 4.7, and 4.8, the peak slips of the beam specimens are observed and the average values are presented in Table 4.2 above. Results of the average maximum strains are computed from the peak slips over the 12-inch embedded length of the steel bar and are presented in the same table. The strains computed are a direct correlation to the steel rebar's yield strain since the difference in the dial gages measurements record the elongation in the rebar.

Addition of SDA to concrete reduces the slip between the rebar and the concrete. The trend of the results also indicates a decrease in the slip length and strain with an increase in the SDA. This could be as a result of an increased frictional resistance that the SDA offers the concrete.

4.2.6 Compressive Strength of Bond Test Specimens

In determining the bond behavior, a standard compressive strength test (ASTM C192) was performed to determine the actual compressive strength used and investigate its influence on the bond behavior. A standard compressive strength test (ASTM C192) was performed alongside the bond test specimens, on three-sample cylinders per point to determine the actual compressive strength used. The average concrete strengths shown in Table 4.3 indicate that the specimen meet the target design strength requirement of 5700psi.

Table 4.3 28-day Mean Compressive Strengths (psi) for the Bond Test Specimen

SDA content (%)	0%	25%	50%
C. Strength (psi)	5777	6726	5665
Expected B. Strength (psi)	924	1034	973
Actual B. Strength (psi)	912	984	903

The expected bond strength (bond stress) is calculated from the compression-bond relationship illustrated in equation 2.1. Comparison of the measured bond strength/stresses with the expected results indicates a closeness in the range of results, with a greatest variation seen with the specimen with 25% SDA. The closeness in results indicates that the compression-bond strength relationship is still applicable even with SDA concrete. Examining the directly proportionality (compression-bond relationship) in the results illustrated in Table 4.3, the compression strength test confirms the effect that it has on the bond strength of concrete.

4.3 Concrete Durability (Freeze-thaw)

Alternate cycles of freezing and thawing subject concrete to durability concerns, which include mainly two types of deterioration, namely surface scaling and internal cracking. Scaling (loss of small particles of mortar on a concrete surface) is the most frequently observed form of deterioration. However, this research will particularly consider the second form of deterioration: cracking that is caused by the internal pressures generated by the action of frost within the hardened concrete. Among the various factors affecting the resistance of the concrete to frost is the strength of the aggregate-mortar interface and the pore structure of the mortar (Pigeon *et al.* 1995). This research utilizes ASTM C666 to study the effect that SDA has on these factors that determine the freeze-thaw properties of concrete. The method in the standard requires the measurement of the fundamental frequency (and relative dynamic modulus of elasticity) and calculation of the durability factor, whose respective reduction and value are indicators of the extent of internal cracking in concrete specimens (Pigeon *et al.* 1995).

The air entrained mixes utilized for the durability test are moist cured and the test procedure (including freeze-thaw cycling) starts at 28 days after curing. They are subjected to 300 cycles of freezing and thawing as specified in ASTM C666 and periodically tested according to ASTM C215. Each cycle involved two hours for the freezing and thawing respectively, for a total of four hours. The following sub-sections present the average results of three specimen samples of the freeze-thaw durability test and discuss the variations caused by the freeze-thaw cycles in weight change, relative dynamic modulus of elasticity, and the durability factor.

4.3.1 Weight Change

The change in weight (or mass) can be an indicator of deterioration of concrete specimens in instances where surface scaling is observed. As shown in Table 4.4, the results of the present research show negligible variations in the specimen weights, indicating no occurrence of surface scaling. This outcome aligns with the assumptions on which this test (ASTM C666) was designed. The assumptions are based on the fact that internal cracking would be the only expected form of deterioration experienced by air entrained concrete specimens.

Table 4.4 Average Percentage Weight Change of Specimens Over N Cycles

	Average Percentage Weight Change		
N	$\Delta_{0\%}$	$\Delta_{25\%}$	$\Delta_{50\%}$
0	0.00	0.00	0.00
35	0.33	0.43	0.42
70	-0.05	0.00	0.00
105	-0.06	0.08	0.03
140	0.03	-0.05	-0.02
175	-0.04	-0.01	0.02
210	0.03	-0.01	-0.04
245	0.03	0.03	0.04
280	-0.02	-0.01	0.04
300	0.01	0.01	-0.02
(Total Δ=)	0.26	0.46	0.48

Minor variations are observed within the specimens. The SDA specimens exhibit greater mass changes than the control (0% SDA) specimen by about 0.20%. The minor variations in weight gain can likely be attributed to the ingress of water within the internal cracks, and a weight loss can relate to minor abrasion of the concrete.

4.3.2 Freeze-thaw Resistance

The primary measures of deterioration are the relative dynamic modulus of elasticity (RDM) and the durability factor (DF), and they are calculated from the measurements of the fundamental transverse frequency (ASTM C666). A reduction in fundamental frequency, hence a reduction in the RDM, signifies internal disruptions/deteriorations within the concrete due to the alternate cycles of freezing and thawing. All specimens utilized for this test are air entrained and contain an air content of approximately 5%.

Increasing amounts of air entraining admixture are utilized for every increase in SDA content, to achieve a similar 5% air content. The results (Figure 4.9, Table 4.5) of these parameters (RDM and DF) are deduced from the measurements of at least three hammer strike point records of the transverse frequencies (ASTM C215) of air-entrained concrete specimens recorded after every 35 cycles of freezing and thawing until the test reached 300 cycles.

Figure 4.9 shows a general decrease in the RDM with an increase in the number of freeze-thaw cycles, signifying a decrease in the freeze-thaw resistance of the concrete over time. The trend indicates a close relationship between the samples with 25% and 50% SDA, but compared to the control specimen, the concrete specimen with 50% SDA provides a slightly higher freeze-thaw resistance after 300 cycles. Overall, the SDA appears to slightly reduce the freeze-thaw resistance of the concrete.

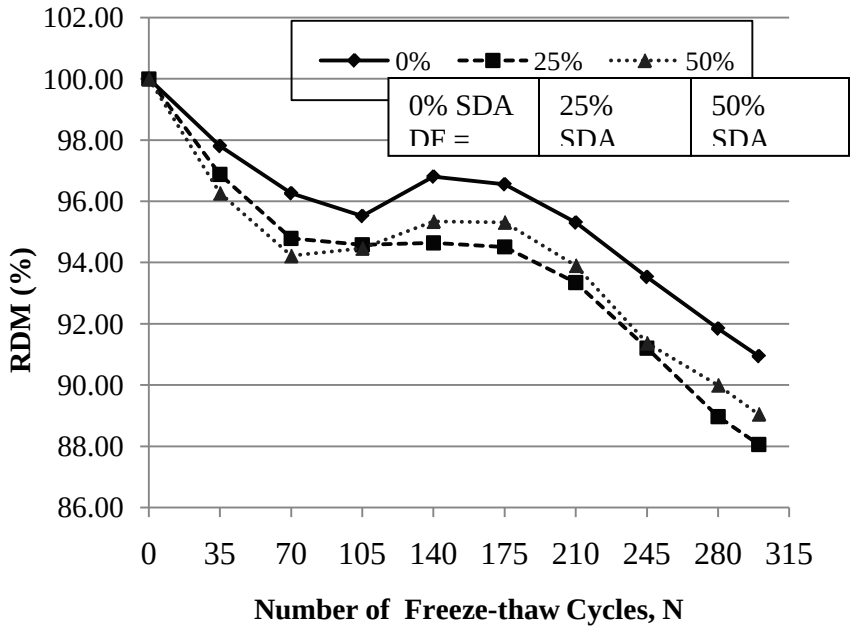

Figure 4.9 Change in RDM (%) of SDA Concrete vs. Number of Cycles

Table 4.5 shows the computed durability factors, which exceed 85% of contrasted threshold (Wang 2009); furthermore, the relative durability factors exceed the 80% threshold defined by ASTM C260. The concrete specimens all possess excellent resistance to freeze-thaw, based on the RDF limits of ASTM C260.

Table 4.5 Durability Factors and Relative Durability Factors

SDA (%) in concrete	Durability Factor, %	Relative Durability Factor (RDF),%
0%	90.940	(ref)
25%	88.057	96.8%
50%	89.045	97.9%

The variation between the SDA concrete specimens is rather insignificant, and it is therefore difficult to determine or recommend the most favorable SDA content for use in concrete. Hence comparison is made between concrete with and without SDA, which indicates that utilizing SDA in concrete would provide a slight decrease in the freeze-thaw resistance of the concrete when designed at the same air content.

4.4 Concrete Corrosion

An important part of this research is to evaluate the corrosion performance of the rebar embedded in the SDA concrete and to determine whether the SDA inhibits or accelerates the corrosion activity of steel in concrete. This evaluation was conducted in accordance to ASTM G109, which calls for measuring the half cell (corrosion) potential and the voltage drop across the 100-Ω resistor placed across the bottom (cathode) and top rebars (anode), whose results aid in determining the total integrated macrocell current and the steel's total corrosion. Potential measurements are generally used to determine corrosion of steel embedded in concrete and also provide a semi-quantitative indication regarding corrosion in the sodium chloride (NaCl) corrosive medium. The total corrosion (metal loss) is a measure of the thickness of the bar lost to corrosion and a direct indicator of the extent of chloride ion penetration through the concrete, while the total macrocell integrated current is a measure of the rate of corrosion activity due to the

macrocell. This section discusses the results of the potential and current measurements and uses them to analyze the effect that SDA has on the corrosion property of concrete.

Beam specimens prepared as described in Section 3 were moist cured for 28 days, and later were subjected to 14 days of soaking in 3% sodium chloride (NaCl) solution followed by 14 days of drying. The NaCl solution provides a necessary ion path in the corrosion reaction of the specimen. The tests were carried out through five soak-dry cycles, and electrical potentials were measured across a 100-Ω resistor after each cycle between the top and bottom steel bars and against a silver nitrate ($AgNO_3$) half cell reference electrode (ASTM C876) using a voltmeter. At the end of the testing, concrete samples were collected from the specimens and the chloride content of the concrete was measured.

4.4.1 Chloride Ion Penetration (Total Corrosion)

The penetration of chloride ions is a function of the permeability of concrete and a measure of the total corrosion experienced by the steel. The water-cementitious ratio is the major factor that governs the permeability of concrete. Among other factors that play a significant role in determining the permeability of concrete is the cement/material specification. Therefore, this section discusses the effect that SDA would likely have on the permeability of concrete and thus the damage of structures subjected to chloride environments. A corrosion test (ASTM G109) was carried out to investigate this property, and presented in Table 4.6 are the average results of three sample reinforced concrete beam specimens carried out over five months for each point containing 0%, 25%, and 50% SDA in concrete.

Table 4.6 Average Corrosion Potentials (Against Reference Electrode) of Specimens

SDA Content (%)	**0%**	**25%**	**50%**
Time (days)	**Half cell (Corrosion) Potential (mV)**		
0	0.00	0.00	0.00
28	-256.82	-276.11	-272.30
56	-183.90	-195.99	-219.91
84	-161.42	-163.68	-145.90
112	-144.47	-202.30	-150.50
140	-135.33	-232.37	-167.07

The results (Table 4.6) indicate that the steel bar embedded in the control specimen has decreasing negative potentials over the whole testing period, whereas the specimens with SDA have decreasing negative potentials for the first 84 days of soaking but later show slightly increased potentials. The large negative values indicate corrosion is beginning to occur (transition state), while the smaller negatives (less than -200mV) indicate no occurrence of corrosion.

Despite initially high values for the half-cell potentials (ranging between -200 and -350 mV for individual specimens), when compared against the values in Table 4.7 the measured potentials generally indicate only a 10% probability of the formation of corrosion cells on the reinforcing steel (ASTM C876). For the given short period of testing, the results indicate that corrosion activity has not yet initiated and the concrete specimens can be said to be in a passive state.

Table 4.7 Probability of Corrosion (ASTM C876)

E (mV_{ref})	Probability of corrosion	Corrosion state
More positive than -200mV	10%	Passive corrosion
Range -200 to -350 mV	uncertain	transition
More negative than -350mV	90%	Active corrosion

In spite of the absence of active corrosion activity, Figure 4.10 illustrates the variations of the resistance of chloride ions (total corrosion) with time. The specimens experience moderate to high ion penetrability with the specimen containing 25% SDA exhibiting the least resistance (largest chloride ion penetration) to the chlorides. The specimen with 50% SDA exhibits the highest resistance to chloride penetration compared to the control specimen, hence offering the best performance for corrosion resistance.

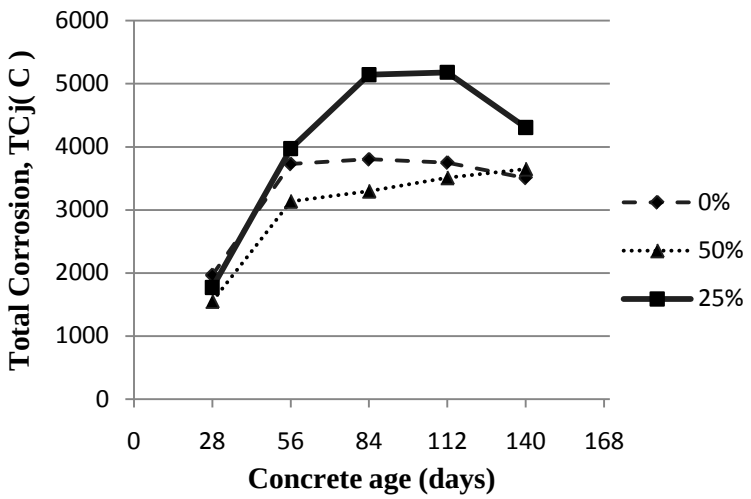

Figure 4.10 Total Corrosion vs. Concrete Age

Figure 4.10 shows that large (50%) SDA contents increase the chloride inhibition properties of concrete. It was expected that an increased SDA content would inadvertently decrease the resistance of the concrete to chloride penetration. This is because the fineness of fly ash (and SDA) has been seen to provide added impermeability to the property of concrete (Crouch *et al.* 2009).

4.4.2 Rate of Corrosion Activity

This sub-section addresses results of the measurements of the macrocell corrosion current between the top and bottom steel bars embedded in concrete and investigates the rate of corrosion of the steel bars over time. The corrosion rate (how fast or slow corrosion is occurring over time) depends on the amount of current flowing through the macrocell specimen with corroding (anode) and cathodic members and gives a quantitative indication of the corrosion tendency of the test specimen (Figure 4.11).

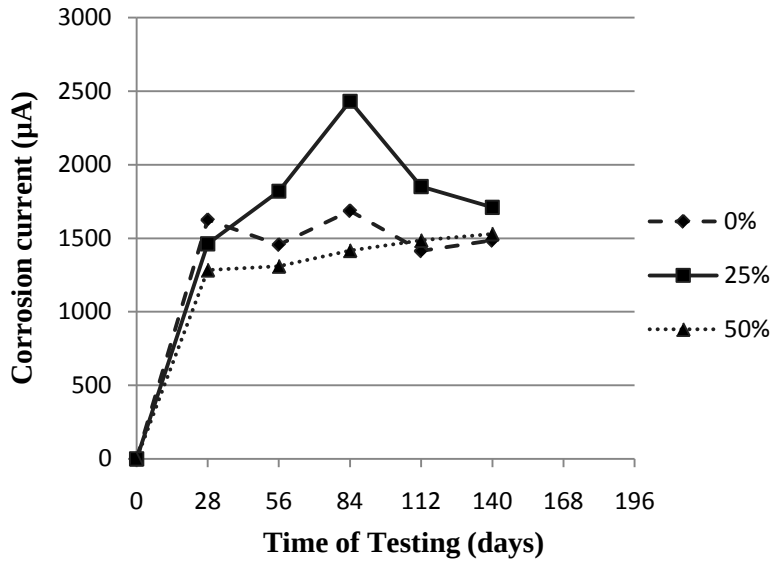

Figure 4.11 Macrocell Current vs. Time of Testing (Corrosion Rate)

The results from the specimens with 25% SDA illustrate an initial steep increase in the slope of curve (corrosion rate) for the first three months indicating a high rate of corrosion activity. The rate of corrosion activity after three months drops significantly. The control specimen presents a fluctuating and a relatively steady rate of corrosion activity.

The results also show a steady and low increase in the macrocell current for the concrete specimen with 50% SDA, indicating that the replacement of 50% SDA in concrete provides a relatively low corrosion rate. This would be expected, given that SDA is a much finer material than cement, hence would provide a low chloride permeable material that would inhibit the rate of corrosion.

4.4.3 Acid Soluble Chloride Content

To measure the corrosion potentials and macrocell current, samples of concrete were taken from the corrosion specimens and tested following ASTM C1152 to measure the total chloride content of the concrete. This test allows for direct comparison of the amount of chloride ions penetrating the different concrete mixes. Samples of concrete were taken at the top, center, and bottom of the corrosion specimens. When possible, three repetitions of the titration were conducted. In four of nine cases, the quantity of concrete collected only allowed for two. The quantities of $AgNO_3$ required to reach the equivalence point for all specimens are provided in Appendix E.

Table 4.8 shows the average quantity of $AgNO_3$ required for each sample of concrete and the corresponding percent of chloride ions present in the concrete. Two types of calculations are shown in this table. Column 4 shows chloride concentrations calculated using equation (3.5) with V_2 equal to 2.971 mL. In this case, some concentrations are very slightly negative, which is not physically possible but relates to small inaccuracies in the experimental procedure. Column 5 shows the concentrations calculated with V_2 equal to 0 mL. The ASTM standard permits this calculation for non-referee analysis, and it is appropriate in this case because comparison is only made between samples used in the present research.

Table 4.8 Results of Acid-Soluble Chloride Testing

Concrete Mix	Sample Location	$AgNO_3$ to reach Equivalence (mL)	%Chloride Ions by Mass of Concrete V_2=2.971 mL	%Chloride Ions by Mass of Concrete V_2=0 mL
	Top	8.322	0.0948	0.1475
Control	Center	5.061	0.0370	0.0897
	Bottom	2.482	-0.0087	0.0440
	Top	5.466	0.0442	0.0969
25% SDA	Center	2.527	-0.0079	0.0448
	Bottom	2.519	-0.0080	0.0447
	Top	6.343	0.0598	0.1124
50% SDA	Center	3.147	0.0031	0.0558
	Bottom	2.246	-0.0128	0.0398

The contours of chloride ion penetration (from column 5) for the three mixes are plotted in Figure 4.12. This chart clearly shows that the chloride ion content in the control specimen is greater than the chloride contents in either the 25% or 50% SDA concretes at the top and center of the specimens. The concentration in all three specimens is very low at the bottom of the specimens.

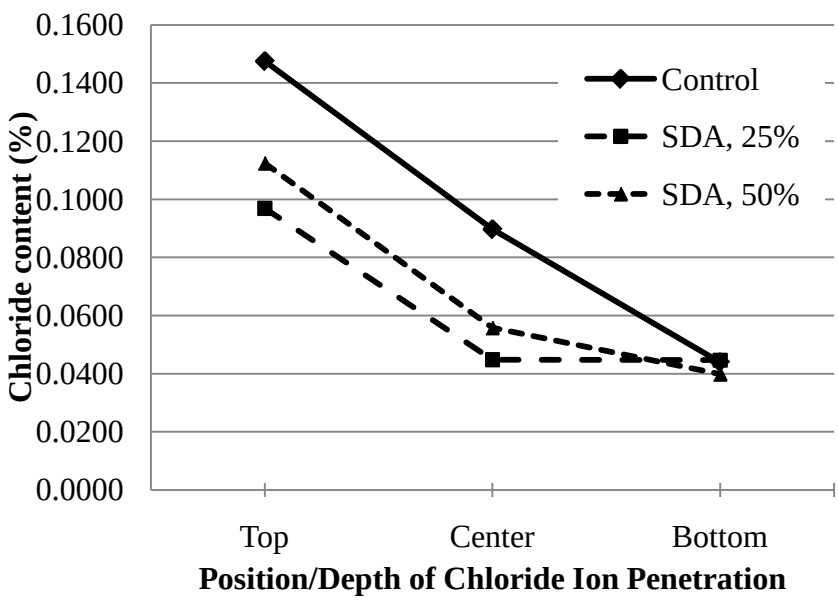

Figure 4.12 Chloride Content (% Mass of Concrete) vs. Depth

The reduced chloride concentrations in the SDA concrete are anticipated because the small particle size of the SDA should produce a more dense concrete that is more resistive to the penetration of water and ions. However, these results are interesting in that the 25% SDA concrete shows a slightly lower degree of penetration than the 50% SDA concrete. There appears to be a limit in the amount of benefit to be gained by the addition of SDA. These results also deviate from the corrosion potential and macrocell current measurements, where the 50% SDA mix appears superior, making a firm conclusion difficult to reach. Based on assessment of all results, it appears the addition of SDA may provide a small amount of benefit in concrete's ability to prevent chloride-induced corrosion.

5. RECOMMENDATIONS AND CONCLUSIONS

5.1 Conclusions

This report investigates the potential for valuable utilization of SDA and its performance in structural concrete. Experimental work was carried out to determine the effect that SDA has on the compressive and bond strength of concrete, its freeze-thaw durability, and its corrosion inhibition properties on steel rebar embedded in concrete. Mixes with varying amounts of SDA were designed and tested in the accordance to the appropriate ASTM standards.

In general, the addition of SDA provides modest benefits when used in certain proportions, and at the very least it did not seem to degrade the properties much. It provides reasonable benefits on the compressive and bond strength when utilized within the optimal limits. Despite the need for more air entrainer, utilization of SDA produces a negligible effect on the freeze-thaw durability of the concrete while an increase in the SDA provides an increased corrosion resistance and a reduced corrosion rate in concrete. Based on the results of this research, SDA has great potential for its utilization as a structural material in transportation infrastructures. The following conclusions can be drawn from the results of this research.

5.1.1 Compressive Strength

Replacement of cement in concrete by SDA generally increases the ultimate strength of the concrete. Generally, the strength attained at 28 and 56 days by concretes containing SDA superseded the strength attained by the control (standard) concrete, indicating an added benefit of about 4-18% and 6-15% respectively, on the ultimate strength gain of concrete.

The results of this study do not indicate at which point the continued replacement of cement with SDA causes the compressive strength to decline below the strength observed from the control (standard) concrete.

A 25-35% SDA replacement provides the best strength results of about 400-650 psi in excess of the target strength at 28 days and about 1350-1800 psi at 56 days. Beyond 35% SDA replacement, the ultimate compressive strength decreases, but mixes with higher replacement percentages still reach the desired design strength.

Replacement of cement with SDA reduces the rate of early strength development/gain. Generally, concrete with SDA exhibits an initial low strength development for the first three days but has its strength accelerate steadily after that time.

5.1.2 Bond Strength

The addition of SDA to concrete provides an increase in bond strength of concrete, in comparison to the control specimen, although the variations of 12% (for 25% SDA) and 5% (for 50% SDA) are relatively small. However, from the trend it is uncertain at what SDA percentage the bond strength will drop below that of the control specimen.

The optimal results in bond strength are attained when SDA utilized in concrete is limited to 25% replacement. Doubling this quantity of SDA (50%) results in reduced variations (decreased bond strength compared to the control). Utilization of SDA provides a worse bond-slip behavior than plain concrete with an increase in the SDA content.

The compression-bond relationship is a direct proportionality (equation 2.1), and the compressive strength test results confirm its effect on the bond strength of concrete. The test also confirms that the relationship (equation 2.1) is still applicable to SDA concrete.

5.1.3 Freeze-thaw (Durability)

More air entraining admixture is required for increasing amounts of SDA replacement to achieve the same air content in concrete. The dosages required in SDA concrete do exceed those used in plain concrete by more than half.

Minor variations in the weight changes of the specimen have a negligible effect on the results on the freeze-thaw testing.

The relative dynamic modulus of elasticity (RDM) of concrete generally decreases with an increase in the freeze-thaw cycles, indicating a decrease in the freeze-thaw resistance of the concrete over time. Concrete specimens with 50% SDA provide a slightly higher freeze-thaw resistance than the specimens with 25% SDA when compared to the control, although the variations between the SDA concrete specimens are relatively small. It is, therefore, difficult to determine or recommend the most favorable SDA content for use in concrete. Hence, comparison is made between concrete with and without SDA, which otherwise indicates that SDA in concrete offers a lower freeze-thaw resistance than the control concrete.

Utilizing SDA in concrete provides a slight decrease in the durability factor, indicating a negligible effect on the freeze-thaw resistance (durability) of the concrete when designed at the same air content.

5.1.4 Corrosion

For the given short period of testing, the results indicate a 10% probability of corrosion (formation of corrosion cells on the reinforcing steel). Active corrosion has not yet been instigated, and the concrete specimens are considered to be in a passive state.

In spite of the absence of active corrosion activity, the specimen with 50% SDA offers the best performance for corrosion resistance. It exhibits the highest resistance to chloride penetration in the half cell potential tests, and show fairly low values of chloride penetration in the direct measurement of acid-soluble chlorides.

5.2 Recommendations

In utilizing SDA, the concrete industry does continue to recognize the importance of sustainable development and the potential benefits that this material has to offer. This research provides an introduction to a clearer understanding of the behavior and performance of this SDA material when used in concrete, and the recommendations outlined below are proposed to complement this work.

Given the potential for the valuable use of spray dryer ash (SDA) and fly ash in general, its beneficial properties, and the likely increase in its production, it is paramount that further research be carried out to better understand the variable aspects and properties of this material.

Before this material can be routinely used, additional research should be carried out to investigate other essential properties of the material, such as the dry density, stiffness, flexural strength, toughness, abrasion resistance, sulfate resistance, and other long-term durability concerns. Other environmental

performance and field handling characteristics need to be further investigated, and quality control measures designed, to ensure its standard application. After considering its structural performance and characteristics in totality, a design standard would be appropriate and useful for future use.

The tests carried out in this research require further in-depth study to determine the trends and behavior of the material when more variable points are considered. In particular, the corrosion test would require a longer duration to clearly establish the corrosion inhibition properties of the concrete. It is also recommended that more study be carried out to determine the behavior of concrete when larger quantities of SDA replacements, in excess of 50%, are used.

It is also recommended that a more detailed understanding of the SDA material is required to critically understand the physical, chemical, and mineralogical properties of the material and its variations in properties due to the variable processing methodologies utilized at the various coal plants. Additional studies on the use of supplemental chemical activation materials, such as lime and alkali compounds, could also be useful in improving the performance of the material.

This research focuses on the positive utility of the SDA in general, and very little concern is given to the high sulfur content. The effect of the high sulfur content should be further investigated, and its role in hardened concrete and non-structural applications should also be determined.

6. REFERENCES

AASHTO. (1994). AASHTO LRFD Bridge Design Specifications. Washington, D.C: American Association of State Highway and Transportation Officials.

AASHTO. (2009). T196 Air Content of Freshly Mixed Concrete by the Volumetric Method. Washington, D.C: American Association of State Highway and Transportation Officials.

ACI Committee 211. (1991). 211.1-91Standard Practice for Selecting Proportions for Normal, Height weight and Mass Concrete. ACI Manual of Concrete Practice, Part 1. Detroit, Michigan: American Concrete Institute.

ACI Committee 211. (1996). 211.4R-93Guide for Selecting Properties for High-Strength Concrete with Portland Cement and Fly Ash. ACI Manual of Concrete Practice, Part 1. Detroit, Michigan: American Concrete Institute.

ACI Committee 318. (2008). Building Code Requirements for Structural Concrete ACI Standard 318-08. Detroit, Michigan: American Concrete Institute.

American Coal Ash Association (ACAA). (2010). CCP Production and Use Statistics. Accessed at http://www.acaa-usa.org/displaycommon.cfm?an=1&subarticlenbr=3 (Feb 09, 2010).

American Coal Ash Association (ACAA). (2007). CCP Production and Use Survey Data. Accessed online at http://www.epa.gov/waste/partnerships/c2p2/use/index.htm (Nov 02, 2009).

American Coal Ash Association (ACAA). (2009). Facts About Coal Ash. Accessed online at www.coalashfacts.org (Nov 02, 2009).

ASTM Standard A944. (2005). Standard Test Method for Comparing Bond Strength of Steel Reinforcing Bars to Concrete using Beam-End Specimen. West Conshohocken, Pennsylvania: ASTM International.

ASTM Standard C125. (2009). Standard Terminology relating to Concrete and Concrete Aggregate. West Conshohocken, Pennsylvania: ASTM International.

ASTM Standard C150. (2009). Standard Specification for Portland Cement. West Conshohocken, Pennsylvania: ASTM International.

ASTM Standard C173. (2009). Standard Test Method for Air Content of Freshly Mixed Concrete, Volumetric Method. West Conshohocken, Pennsylvania: ASTM International.

ASTM Standard C192. (2006). Standard Practice for Making and Curing Concrete Test Specimens in the Laboratory. West Conshohocken, Pennsylvania: ASTM International.

ASTM Standard C215. (2009). Standard Test Method for Fundamental Transverse, Longitudinal, and Torsional Frequencies of Concrete Specimens. West Conshohocken, Pennsylvania: ASTM International.

ASTM Standard C618. (2008). Standard Specification for Fly Ash and Raw or Calcined Natural Pozzolan for Use as Mineral Admixture in Concrete, West Conshohocken, Pennsylvania: ASTM International.

ASTM Standard C666. (2003). Standard Test Method for Resistance of Concrete to Rapid Freezing and Thawing. West Conshohocken, Pennsylvania: ASTM International.

ASTM Standard C876. (2009). Standard Test Method for Corrosion Potentials of Uncoated Reinforcing Steel in Concrete. West Conshohocken, Pennsylvania: ASTM International.

ASTM Standard C1152. (2009). Standard Test Method for Acid-Soluble Chloride in Mortar and Concrete. West Conshohocken, Pennsylvania: ASTM International.

ASTM Standard G59. (1999). Standard Test Method for Conducting Potentiodynamic Polarization Resistance Measurements. West Conshohocken, Pennsylvania: ASTM International.

ASTM Standard G106. (1999). Standard Practice for Verification of Algorithm and Equipment for Electrochemical Impedance Measurements. West Conshohocken, Pennsylvania: ASTM International.

ASTM Standard G109. (1999). Standard Test Method for Determining the effects of Chemical Admixtures on the Corrosion of Embedded Steel Reinforcement in Concrete Exposed to Chloride Environments. West Conshohocken, Pennsylvania: ASTM International.

Babcock and Wilcox. (1978). Steam: Its Generation and Use. New York: New York, Appendices.

Bavarian, B. and Reiner, L. (2006). Current Progress in Corrosion Inhibition of Reinforcing Steel in Concrete using Migrating Corrosion Inhibitors. San Diego, California: California State University.

Berry, M., Cross, D., and Stephens, J. (2009). Changing the Environment: An Alternative 'Green' Concrete produced without Portland Cement. 2009 World of Coal Ash Conference, Lexington, Kentucky, May 4-7.

Buck, A. D. (1977). Recycled Concrete as a Source of Aggregate. *ACI Journal Proceedings*, 74 (5), pp. 212-219.

Burden, D. (2006). The Durability of Concrete Containing High Levels of Fly Ash. New Brunswick, Canada: University of New Brunswick.

Bye, G.C. (1999). Portland Cement. London, UK: Thomas Telford Publishing.

CDOT. (2008). Concrete Table: Standard Specifications for Road and Bridge Construction. Colorado Department of Transportation.

Chang, E. H. (2009). Shear and Bond Behavior of Fly-Ash Based Geo-Polymer Concrete Beams. Curtin University of Technology.

Cross, D., Stephens, J., and Vollmer, J. (2005). Structural Applications of 100 Percent Fly Ash Concrete. 2005 World of Coal Ash Conference, Lexington, Kentucky, April 11-15.

Crouch, L.K. and Philips, J. (2009). Lean, Green and Mean Concrete. 2009 World of Coal Ash Conference, Lexington, Kentucky, May 4-7.

Daigle, L. and Lounis, Z. (2006). Life Cycle Cost Analysis of High Performance Concrete Bridges Considering Their Environmental Impacts. Ottawa Canada: Institute for Research in Construction, National Research Council.

Eligehausen, R., Bertero, V., and Popov, E. (1983). Local Bond Stress-Slip Relationships of Deformed Bars Under Generalized Excitations. Earthquake Engineering Research Center, Report no. 83-23, University of California, Berkeley, CA.

Elsageer, M. A., Milliard, S. G. and Barnett, S. J. (2009). Strength Development of Concrete Containing Coal Fly Ash under Different Curing Conditions. 2009 World of Coal Ash Conference, Lexington, Kentucky, May 4-7.

EPRI. (2007). A Review of Literature Related to the Use of Spray Dryer Absorber Material; Production, Characterization, Utilization Applications, Barriers, and Recommendations. Electric Power Research Institute, TR1014915.

EPRI. (1998). Coal Ash: Its Origin, Disposal, Use and Potential Health issues. Environmental Focus, Issue Report Electric Power Research Institute, BR-111026.

Federal Highway Administration. (2009). FHWA Bridge Programs - Material Type of Structure by State. Accessed online at http://www.fhwa.dot.gov/bridge/material.cfm (July 30, 2010).

Garshol, F.K. and Lacerda, L. (2007). Shotcrete Corner: Watertight Permanent Shotcrete Linings in Tunneling and Underground Construction. American Shotcrete Association.

Golden, D.M. and DiGioia, A. M. (2003). Fly Ash for Highway Construction and Development. USEPA Case Study No.10.

Hoffman, G. K. (no date). Western Region Fly Ash Survey. Socorro, New Mexico: New Mexico Bureau of Mines and Mineral Resources.

Joshi, R.C. and Lohtia, R.P. (1997). Fly Ash in Concrete: Production, Properties and Uses. London, UK: Taylor & Francis Group.

King, B. (2005). Making Better Concrete: Guidelines to using Fly Ash for Higher Quality, Eco-friendly Structures. California: Green Building Press.

Kosmatka, S.H., Kerkhoff, B., and Panarese, W.C. (2002). Design and Control of Concrete Mixtures. Portland Cement Association.

Kumar, B., Tike, J. K., and Nanda, P. K. (2007). Evaluation of properties of High Volume Fly Ash for Concrete Pavements. *ASCE Journal of Materials in Civil Engineering*, 19(10), pp. 906-911.

Lowes, L.N., Moehle, J.P., and Govindjee, S. (2004). A Concrete-Steel Bond Model for Use in Finite Element Modeling of Reinforced Concrete Structures, *ACI Structural Journal*, 101(4), pp. 501-511.

Maggenti, R. (2009). Green Mass Concrete for San Francisco Bay. HPC Bridge Views, Issue 57, Sept. /Oct. 2009.

Malhotra, V.M. (1986). Fly Ash, Silica Fume, Slag and Natural Pozzolans in Concrete: Proceedings-Second International Conference. Farmington Hills, MI, American Concrete Institute.

Nawy, G. E. (2000). Reinforced Concrete: A Fundamental Approach, 4th edition. New Jersey: Prentice Hall.

Neville A. (2006). Concrete. London, UK: Thomas Telford.

PCA. (2002). Types and Causes of Concrete Deterioration, Concrete Technology, CIS536, Portland Cement Association, Skokie, Illinois.

PCA. (2006). A History of Cement, Portland Cement Association, Skokie, Illinois.

PCA. (2009). Building Green with Concrete Portland Cement Association. Accessed online at http://www.cement.org/buildings/green_leed (Nov 12, 2009).

PCA. (2009a). Highways Portland Cement Association. Accessed online at http://www.cement.org/pavements/pv_cp_highways.asp (Nov 10, 2009).

PCA. (2009b). Highways Portland Cement Association. Accessed online at http://www.cement.org/buildings/ (Nov 10, 2009).

Pigeon, M. and Pleau, R. (1995). Durability of Concrete in Cold Climates. London, UK: E & FN Spon.

Poutos, K.H., Alani, A.M., Walden, P.J., and Sangha, C.M.. (2008). Relative Temperature Changes within Concrete Made with Recycled Glass Aggregate. *Construction and Building Materials*, 22(4), pp. 557-565.

Richardson, G. M. (2002). Fundamentals of Durable Reinforced Concrete. New York: New York Spon.

Russell, L. H, Borax Technologies, and Folliard, K. (Fall 2006). The Impact of Fly Ash on Air Entrained Concrete. Tech Talk: University of Texas.

Sharp, R.S. (2004). Evaluation of Two Corrosion Inhibitors using Two Application Methods for Reinforced Concrete Structures. Charlotteville, Virginia: Virginia Transportation Research Council.

Smith, P. (2006). Fly Ash: A Nuisance Dust worth its Weight in Cement, *Concrete News*, Summer.

Tempest, B., Sanusi, O., Gergely, J., Ogunro, V., and Weggel, D. (2009). Optimization of Fly Ash based Geopolymer Concrete by Measurement of Free Hydroxyl Ions. 2009 World of Coal Ash Conference, Lexington, Kentucky, May 4-7.

Tonias, D.E. and Zhao, J.J. (2007). Bridge Engineering, Design, Rehabilitation and Maintenance of Modern Highway Bridges, 2nd Edition. New York: McGraw Hill.

TRB. (2009). Concrete Bridges. Transportation Research Board A2C03 Committee on Concrete Bridges. Accessed online at http://onlinepubs.trb.org/onlinepubs/millennium/00019.pdf (Dec 10, 2009).

Trejo, D., Folliard, K. J. and Du,L. (2004). Sustainable Development using Controlled Low-Strength Material. International Workshop on Sustainable Development and Concrete Technology, Tsinghua University, Beijing,China, May 20-21.

US Geological Survey. (2008). Mineral Commodities Summary: Cement. Accessed online at http://minerals.usgs.gov/minerals/pubs/commodity/cement/mcs-2008-cemen.pdf (Nov 12, 2009).

Wang, K. (2009). Freeze-thaw Durability of Low Permeability Concrete. Ames, Iowa: Institute for Transportation, Iowa State University.

Wipf, J. T. (2006). Evaluation of Corrosion Resistance of the Different Steel Reinforcement Types. Ames, Iowa: Bridge Engineering Center, Iowa State University.

APPENDIX A: MIX DESIGN

(PCA Absolute Volume Method (Komastka *et al*. 2002) for a cubic yard)

Constituent Material	Description	Specific Gravity	Moisture Content(%)	Bulk Unit Wt (pcf)	Fineness Modulus
Cement	Type I, ASTM C150	3.15	NA	NA	NA
Coarse Aggregate	Well-graded, 3/4" max. size	2.68	2.00		NA
Fine Aggregate	Natural sand (ASTM C33)	2.64	1.00		2.80

Density of water =	62.4	pcf	
Desired compressive strength =	4500	psi	
Required mean compressive strength =	5700	psi	(reference Table 9-11)
Water/cement ratio =	0.525		(interpolated from Table 9-3, note maximum from Table 9-1)
Air content =	2	%	(entrapped air based on Table 9-5; we will not use air-entrainment)
Slump desired =	1	in	(based on Table 9-6)
Water content =	340	lb	(for a cubic yard of concrete, based on Table 9-5)
Cement content =	648	lb	(water content)/(w/c ratio)
Coarse aggregate content =	1674	lb	(based on Table 9-4),(unit weight in pcf) *($27ft^3/yd^3$) * (bulk volume)
Admixture content =	0	fl oz	

Determining fine aggregate content by volume:

Water =	5.45	ft^3	(content in lbs)/(specific gravity x density of water)
Cement =	3.29	ft^3	(content in lbs)/(specific gravity x density of water)
Air =	0.54	ft^3	(percent/100 x 27 ft^3)
Coarse aggregate =	10.03	ft^3	(content in lbs)/(specific gravity x density of water)

Total - fine aggregate =	19.31	ft^3	
Fine aggregate =	7.69	ft^3	[27 - (total - fine aggregate)]
Fine-aggregate content =	1267	lb	(volume x specific gravity x density of water)

Corrections for moisture content of aggregates:

Coarse aggregate =	1707	lb	(weight x (1 + MC/100))
Fine aggregate =	1280	lb	(weight x (1 + MC/100))
Water =	16.25	lb	(weight of water) - (CA dry weight x MC/100) - (FA dry weight x MC/100)
			(reference page 164)

Final weights for one cubic yard of concrete:

Water =	324	lb
Cement =	648	lb
Coarse aggregate =	1707	lb
Fine aggregate =	1280	lb

Final weights for indicated cubic feet of concrete:

Cubic feet of concrete desired =	0.2	ft^3
Water =	2.4	lb
Cement =	4.8	lb
Coarse aggregate =	12.65	lb
Fine aggregate =	9.5	lb

APPENDIX B: COMPRESSIVE STRENGTH RESULTS

	Day 3			Day 7			Day 14			Day 28			Day 56		
Mix type	Load (kips)	Strength (psi)	Mean strength (psi)	Load (kips)	Strength (psi)	Mean strength (psi)	Load (kips)	Strength (psi)	Mean strength (psi)	Load (kips)	Strength (psi)	Mean strength (psi)	Load (kips)	Strength (psi)	Mean strength (psi)
Control (C)	123,000	4,350	4,461	150,000	5,305	5,084	157,500	5,570	5,623	171,000	6,048	5,765	184,500	6,525	6,428
	120,750	4,271		138,750	4,907		160,500	5,677		156,000	5,517		180,750	6,393	
	134,625	4,761		142,500	5,040		159,000	5,623		162,000	5,730		180,000	6,366	
Mix 1 (15%)	102,750	3,634	3,997	153,750	5,438	4,518	152,250	5,385	5,243	168,750	5,968	5,650	168,000	5,942	6,225
	120,750	4,271		129,000	4,562		157,500	5,570		151,500	5,358		175,500	6,207	
	115,500	4,085		100,500	3,554		135,000	4,775		159,000	5,623		184,500	6,525	
Mix 2 (20%)	112,500	3,979	3,814	148,000	5,234	5,175	165,000	5,836	6,166	182,000	6,437	6,514	210,000	7,427	7,132
	105,000	3,714		145,000	5,128		178,000	6,295		185,000	6,543		200,000	7,074	
	106,000	3,749		146,000	5,164		180,000	6,366		185,500	6,561		195,000	6,897	
Mix 3 (25%)	102,500	3,625	3,690	145,000	5,128	5,270	172,500	6,101	5,865	175,000	6,189	6,154	197,500	6,985	7,050
	103,000	3,643		147,000	5,199		160,000	5,659		176,000	6,225		200,500	7,091	
	107,500	3,802		155,000	5,482		165,000	5,836		171,000	6,048		200,000	7,074	
Mix 4 (30%)	105,000	3,714	3,802	153,000	5,411	5,341	158,000	5,588	5,647	190,500	6,738	6,808	210,000	7,427	7,262
	110,000	3,890		147,000	5,199		161,000	5,694		195,000	6,897		198,000	7,003	
	107,500	3,802		153,000	5,411		160,000	5,659		192,000	6,791		208,000	7,356	
Mix 5 (35%)	110,000	3,890	3,737	156,000	5,517	5,270	147,500	5,217	5,535	180,000	6,366	6,366	210,000	7,427	7,516
	107,000	3,784		141,000	4,987		160,500	5,677		180,000	6,366		217,500	7,692	
	100,000	3,537		150,000	5,305		161,500	5,712		180,000	6,366		210,000	7,427	

Mix 6 (40%)	70,000	2,476	2,499	120,000	4,244	4,492	152,500	5,394	5,199	175,000	6,189	6,130	196,000	6,932	6,891
	70,000	2,476		131,000	4,633		148,500	5,252		182,500	6,455		187,500	6,631	
	72,000	2,546		130,000	4,598		140,000	4,951		162,500	5,747		201,000	7,109	
Mix 7 (45%)	50,000	1,768	1,933	120,000	4,244	4,209	141,000	4,987	5,111	165,000	5,836	5,977	185,000	6,543	6,602
	53,000	1,874		118,000	4,173		145,000	5,128		175,000	6,189		185,000	6,543	
	61,000	2,157		119,000	4,209		147,500	5,217		167,000	5,906		190,000	6,720	
Mix 8 (50%)	50,000	1,768	1,857	115,000	4,067	3,896	135,000	4,775	4,769	161,000	5,694	5,541	198,000	7,003	6,861
	61,500	2,175		105,500	3,731		135,000	4,775		146,000	5,164		180,000	6,366	
	46,000	1,627		110,000	3,890		134,500	4,757		163,000	5,765		204,000	7,215	

APPENDIX C: BOND STRENGTH RESULTS

C-1: COMPRESSIVE STRENGTH RESULTS

SDA Content	0%		25%		50%	
	Load (lbs)	Strength (psi)	Load (lbs)	Strength (psi)	Load (lbs)	Strength (psi)
Specimen 1	169,000	5,977	189,000	6,684	159,000	5,623
Specimen 2	159,000	5,623	190,000	6,720	157,500	5,570
Specimen 3	162,000	5,729	191,500	6,773	164,000	5,800
Average Load	163,333	5,777	190,167	6,726	160,167	5,665

APPENDIX D: FREEZE-THAW RESULTS

D-1: WEIGHTS OF SPECIMENS

	Specimen weights (lbs)								
Number of cycles	**F1**	**F2**	**F3**	**F4**	**F5**	**F6**	**F7**	**F8**	**F9**
0	17.0945	17.2690	17.2575	16.8165	17.3315	17.0905	16.6440	16.5680	16.5145
35	17.1830	17.2790	17.3290	16.8950	17.3990	17.1640	16.6655	16.6600	16.6120
70	17.1890	17.2585	17.3200	16.8880	17.4005	17.1670	16.6920	16.6535	16.5905
105	17.1735	17.2605	17.6050	16.9320	17.4020	17.1625	16.6895	16.6660	16.5945
140	17.1765	17.2620	17.3135	16.8975	17.4020	17.1705	16.6760	16.6705	16.5935
175	17.1700	17.2453	17.3135	16.9030	17.3945	17.1675	16.6790	16.6755	16.5960
210	17.1730	17.2490	17.3200	16.8975	17.3940	17.1680	16.6655	16.6725	16.5930
245	17.1850	17.2530	17.3210	16.9040	17.4005	17.1730	16.6725	16.6780	16.6005
280	17.1885	17.2490	17.3125	16.9103	17.4060	17.1547	16.6741	16.6773	16.6196
300	17.1805	17.2550	17.3175	16.9003	17.4045	17.1662	16.6755	16.6785	16.6080

D-2: TRANSVERSE FREQUENCY SPECIMEN RESULTS

No. of cycles, N	**0**	**35**	**70**	**105**	**140**	**175**	**210**	**245**	**280**	**300**
Frequencies, n	**n**	**n_1**	**n_2**	**n_3**	**n_4**	**n_5**	**n_6**	**n_7**	**n_8**	**n_9**
Specimen	**Transverse Frequencies (Hz) of Specimen**									
F1	2113.827	2082.046	2073.580	2069.592	2077.249	2076.594	2067.357	2044.235	2027.128	2020.531
F2	2108.627	2098.052	2077.139	2074.838	2088.375	2084.751	2061.373	2040.126	2022.174	2010.982
F3	2109.156	2081.596	2061.436	2043.567	2064.042	2060.241	2052.496	2038.934	2018.548	2006.463
F4	2081.460	2047.932	2023.852	2026.220	2023.238	2019.809	2005.575	1988.983	1960.385	1948.248
F5	2093.413	2062.223	2034.641	2029.213	2034.141	2035.677	2024.236	1999.234	1971.732	1962.532
F6	2096.846	2062.817	2047.701	2043.845	2044.014	2041.672	2029.800	2001.278	1983.457	1974.531
F7	1993.339	1947.169	1939.403	1947.342	1960.468	1953.203	1937.064	1919.934	1908.345	1897.564
F8	2063.989	2033.577	2006.201	2005.815	2010.305	2013.207	2002.835	1958.358	1939.002	1931.345
F9	2004.587	1967.230	1938.517	1938.527	1948.033	1951.721	1934.348	1915.458	1902.463	1890.623
	Average Transverse Frequencies (Hz) of Specimen									
0%	2110.537	2087.231	2070.718	2062.666	2076.555	2073.862	2060.409	2041.098	2022.617	2012.659
25%	2090.573	2057.657	2035.398	2033.093	2033.798	2032.386	2019.870	1996.498	1971.858	1961.770
50%	2020.638	1982.659	1961.374	1963.895	1972.935	1972.710	1958.082	1931.250	1916.603	1906.511

D-3: RELATIVE DYNAMIC MODULI OF ELASTICITY (RDM) SPECIMEN RESULTS

N	0	35	70	105	140	175	210	245	280	300	
RDM	P_{n0}	P_{n1}	P_{n2}	P_{n3}	P_{n4}	P_{n5}	P_{n6}	P_{n7}	P_{n8}	P_{c9}	DF
	Specimen Values of Relative Dynamic Modulii of Elasticity (%)										
F1	100.000	97.016	96.228	95.858	96.569	96.508	95.652	93.524	91.965	91.368	91.368
F2	100.000	98.999	97.036	96.821	98.088	97.748	95.568	93.608	91.968	90.953	90.953
F3	100.000	97.404	95.526	93.877	95.768	95.415	94.699	93.452	91.593	90.499	90.499
F4	100.000	96.804	94.541	94.763	94.484	94.164	92.841	91.312	88.705	87.610	87.610
F5	100.000	97.042	94.464	93.961	94.417	94.560	93.500	91.205	88.713	87.887	87.887
F6	100.000	96.781	95.367	95.009	95.024	94.807	93.707	91.092	89.477	88.674	88.674
F7	100.000	95.421	94.662	95.438	96.729	96.014	94.433	92.771	91.654	90.621	90.621
F8	100.000	97.075	94.479	94.442	94.866	95.140	94.162	90.026	88.255	87.560	87.560
F9	100.000	96.308	93.517	93.518	94.437	94.795	93.115	91.305	90.071	88.953	88.953
	Average Values of Relative Dynamic Modulii of Elasticity										
0%	100.000	97.806	96.263	95.519	96.808	96.557	95.306	93.528	91.842	90.940	90.940
25%	100.000	96.876	94.791	94.577	94.642	94.510	93.350	91.203	88.965	88.057	88.057
50%	100.000	96.268	94.219	94.466	95.344	95.316	93.903	91.367	89.993	89.045	89.045

APPENDIX E: CORROSION TEST RESULTS

E-1: SPECIMEN RESULTS AT 28 DAYS

SDA Content	Specimen	Voltage across Resistor, V (mV)	Macrocell Current, I_{28} (µA)	Corrosion Potential (mV_{ref})	Total Corrosion, TC_{28} (C)
0%	CF1	167.99	1,679.90	273.50	2,032.01
	CF2	140.71	1,407.10	264.44	1,701.97
	CF3	178.99	1,789.90	232.53	2,165.06
25%	CF4	176.65	1,766.50	278.14	2,136.76
	CF5	125.00	1,250.00	252.26	1,512.00
	CF6	137.16	1,371.60	297.94	1,659.03
50%	CF7	161.71	1,617.10	273.65	1,956.04
	CF8	107.83	1,078.30	272.75	1,304.25
	CF9	115.57	1,155.70	270.51	1,397.93

E-2: SPECIMEN RESULTS AT 56 DAYS

SDA Content	Specimen	Voltage across Resistor, V (mV)	Macrocell Current, I_{56} (µA)	Corrosion Potential (mV_{ref})	Total Corrosion, TC_{56} (C)
0%	CF1	182.50	1,825.00	209.80	4,239.53
	CF2	150.35	1,503.50	170.62	3,520.60
	CF3	104.10	1,041.00	171.28	3,424.26
25%	CF4	182.31	1,823.10	172.41	4,341.98
	CF5	199.14	1,991.40	193.85	3,920.80
	CF6	164.54	1,645.40	221.70	3,649.30
50%	CF7	161.04	1,610.40	240.70	3,903.98
	CF8	102.22	1,022.20	208.22	2,540.70
	CF9	129.62	1,296.20	210.83	2,965.82

E-3: SPECIMEN RESULTS AT 84 DAYS

SDA Content	Specimen	Voltage across Resistor, V (mV)	Macrocell Current, I_{84} (µA)	Corrosion Potential (mV_{ref})	Total Corrosion, TC_{84} (C)
0%	CF1	63.70*	1,637.00	154.26	4,187.64
	CF2	149.72	1,497.20	126.85	3,629.65
	CF3	92.76*	1,927.60	203.16	3,590.82
25%	CF4	261.00	2,610.00	162.10	5,362.28
	CF5	288.70	2,887.00	143.45	5,900.91
	CF6	179.94	1,799.40	185.49	4,166.83
50%	CF7	180.00	1,800.00	164.57	4,125.22
	CF8	131.22	1,312.20	149.87	2,823.69
	CF9	113.65	1,136.50	123.28	2,942.59

E-4: SPECIMEN RESULTS AT 112 DAYS

SDA Content	Specimen	Voltage across Resistor, V (mV)	Macrocell Current, I_{112} (µA)	Corrosion Potential (mV_{ref})	Total Corrosion, TC_{112} (C)
0%	CF1	67.50*	1,675.00	153.00	4,006.20
	CF2	146.55	1,465.50	147.10	3,583.68
	CF3	110.15	1,101.50	133.30	3,664.00
25%	CF4	162.72	1,627.20	175.60	5,125.32
	CF5	196.10	1,961.00	214.40	5,864.14
	CF6	196.74	1,967.40	216.90	4,556.32
50%	CF7	76.66*	1,766.60	158.60	4,314.16
	CF8	128.50	1,285.00	155.70	3,141.57
	CF9	140.35	1,403.50	137.20	3,072.38

*Omitted from computation of averages

E-5: SPECIMEN RESULTS AT 140 DAYS

SDA Content	Specimen	Voltage across Resistor, V (mV)	Macrocell Current, I_{140} (µA)	Corrosion Potential against Ref.(mV)	Total Corrosion, TC_{140} (C)
0%	CF1	61.30*	1,613.00	112.00	3,977.16
	CF2	139.30	1,393.00	131.10	3,457.64
	CF3	145.00	1,450.00	162.90	3,086.29
25%	CF4	167.30	1,673.00	213.90	3,991.92
	CF5	201.30	2,013.00	246.90	4,806.95
	CF6	144.40	1,444.00	236.30	4,126.43
50%	CF7	68.60*	1,686.00	161.10	4,176.26
	CF8	158.20	1,582.00	164.80	3,467.92
	CF9	132.00	1,320.00	175.30	3,294.35

*Omitted from computation of averages

E-6: RESULTS OF TITRATION TO MEASURE ACID-SOLUBLE CHLORIDE CONTENTS

Blank Determination (water) : 2.971 mL

Concrete:	**Control**			**SDA 25%**			**SDA 50%**		
Location:	Top	Center	Bottom	Top	Center	Bottom	Top	Center	Bottom
	9.347	6.682	2.515	6.525	2.530	2.676	6.104	2.873	2.100
	7.296	3.439	2.448	4.406	2.524	2.650	12.218*	3.685	1.974
		2.779				2.232	6.582	2.882	2.665
Average:	8.322	5.061	2.482	5.466	2.527	2.663	6.343	3.279	2.037

*Omitted from computation of averages